Electrochemistry, 2. Inorganic Electrochemical Processes

ULLMANN'S ENCYCLOPEDIA OF INDUSTRIAL CHEMISTRY

Hartmut Wendt, Technische Hochschule Darmstadt, Darmstadt, Germany

Helmut Vogt, Technische Fachhochschule Berlin, Berlin, Germany

Gerhard Kreysa, Dechema, Frankfurt/Main, Germany

Hubert Goldacker, Forschungszentrum Karlsruhe, Karlsruhe, Germany

Klaus Jüttner, Dechema, Frankfurt/Main, Germany

Ulrich Galla, Forschungszentrum Karlsruhe, ITC-CPV, Karlsruhe, Germany

Helmut Schmieder, Forschungszentrum Karlsruhe, ITC-CPV, Karlsruhe, Germany

Symbols

A:	total electrode area
a_e:	specific electrode area
b:	Tafel slope
d:	electrode – electrode distance (inter-electrode distance); characteristic length
D:	diffusion coefficient
d':	electrode thickness
d_b:	bubble diameter
d_p:	particle diameter
E^0:	standard electrode potential
h:	height of electrode, bed height, heat-transfer coefficient
j:	current density
j^*:	"current concentration"
j_b:	bed current density
j_l:	limiting current density
j_0:	exchange current density
k, k':	electrochemical rate constants
k_m:	mass-transfer coefficient
k_1:	macroconvective mass-transfer coefficient
k_2:	bubble-induced mass-transfer coefficient
L:	electrode length
S:	cross sectional area
STY:	space – time yield
t^+, t^-:	transport numbers
$U_{0,c}$:	equilibrium potential difference of the cell reaction
U_{cell}:	cell voltage
ΔU_Ω:	ohmic voltage drop

DOI: 10.1002/14356007.o09_o03

u: linear flow velocity
V: volume flow rates
v: void fraction; bed voidage
x: distance from electrode; distance along electrode; bed depth
y: flow length
z: number of electrons
Gr: Grasshof number
Nu: Nusselt number
Pr: Prandtl number
Re: Reynolds number
Sc: Schmidt number
Sh: Sherwood number
Wa: Wagner number
α^+, α^-, α: charge-transfer coefficients
δ: thickness of Nernst diffusion layer
η: overpotential; dynamic viscosity
κ: specific conductivity
κ/κ_L: effective conductivity of a dispersion relative to the conductivity of bubble-free liquid
λ: equivalent conductivity
θ: fraction of electrode surface shielded by adhering bubbles
ϕ: potential
ϕ^e: current efficiency
Φ: Thiele modulus
ν: kinematic viscosity
ν_i: stoichiometric number
ϱ: density; resistivity
ω: angular velocity

Subscripts

a: anodic
ad: adsorbed
c: cathodic
conc: concentration
ct: charge transfer
G: gas
L: liquid
m: mean, mass
ox: oxidized species
p: particle
r: rising bubble
red: reduced species
rs: rising swarm of bubbles
s: solution, electrolyte

1. Chlor-Alkali Electrolysis

The products of industrial chlor-alkali electrolysis are of great importance for the chemical industry: chlorine [*7782-50-5*], caustic soda [*1310-73-2*], hypochlorite, chlorate, and perchlorate. The rate of chlorine production is considered one of the measures of the industrial standing of a nation. Of the electrochemical processes, chlor-alkali electrolysis holds second place in total electrical energy consumption, aluminum production consuming more.

In industrial chlor-alkali electrolysis, the electrolyte is generally aqueous sodium chloride solution, to a much lesser extent potassium chloride solution. For the production of sodium metal, fused sodium chloride is used. In all cases, the primary anodic reaction is the oxidation of the chloride ion, in itself a relatively simple reaction,

$$Cl^- \rightarrow \frac{1}{2}\,Cl_2 + e^-$$

but this reaction can be accompanied or followed by other reactions. At the cathode, various reactions can take place: the products depend on the operating conditions. Chlor-alkali electrolysis justifies a detailed survey, not only on account of its economic importance, but also because of the interesting reaction technology. It is an excellent example of the way in which one anode reaction, from one raw material, can lead to a great variety of products, according to the way in which secondary reactions are prevented, encouraged, or controlled by the design of the equipment and choice of the reaction conditions. The introduction of dimensionally stable anodes based on ruthenium oxide – titanium oxide [1], which replaced the conventional graphite anodes in all aqueous chloride electrolyses, has contributed to far-reaching process modifications within the last three decades.

1.1. Molten Salt Electrolysis

In molten salt electrolysis, the cathodic reaction

$$Na^+ + e^- \rightarrow Na$$

yields sodium [*7440-23-5*], which is of lower density than the melt, floats to the surface, and is then easily separated. Futher reaction of the two products does not take place, provided recombination is prevented. The high cell voltage makes the process useful only for winning sodium (→ Sodium and Sodium Alloys). Chlorine is in this sense a byproduct.

1.2. Production of Chlorine

Processes designed to produce chlorine are always based on electrolysis of aqueous chloride solutions, below 100 °C. The decomposition voltage is much lower than that for molten salt electrolytes. This technology is, however, considerably complicated by the secondary reactions of the primary electrolysis products and by side reactions.

The dissolved chlorine formed at the anode reacts with water to form hypochlorite,

$$Cl_2+H_2O\rightarrow HClO+Cl^-+H^+$$

The electrolyte near the anode becomes acidic. If the electrolyte is not replaced, or not replaced quickly enough, the supersaturation of chlorine at the anode increases to such an extent that stable chlorine bubbles form. Acidic electrolyte is the precondition of chlorine gas formation in aqueous solution. If the anode boundary layer is neutralized, the formation of gaseous chlorine is prevented. This situation arises if no steps are taken to prevent mixing of anolyte and catholyte.

At the cathode, hydrogen gas and hydroxyl ions are liberated simultaneously from aqueous solution:

$$2\,H_2O+2\,e^-\rightarrow H_2+2\,OH^-$$

There are two ways of ensuring the formation of gaseous chlorine: one is to prevent the hydroxyl ions from reaching the anode region, the other is to prevent the formation of these ions at the cathode in the first place. Both approaches are used in industry and have led to two technologies. One of these, the mercury process, uses mercury as the cathode material. The other technology uses cells divided by either a diaphragm or a membrane.

Mercury Process. Mercury [*7439-97-6*], the liquid cathode, is able to alloy the liberated sodium forming sodium amalgam (Fig. 1).

$$Na^+ + n\,Hg + e^- \rightarrow NaHg_n$$

The evolution of hydrogen is prevented by the exceptionally high overpotential of hydrogen at mercury surfaces. Hydroxyl ions are not formed. Since the viscosity of amalgam increases strongly with the sodium concentration, the sodium in the liquid alloy must be kept below about

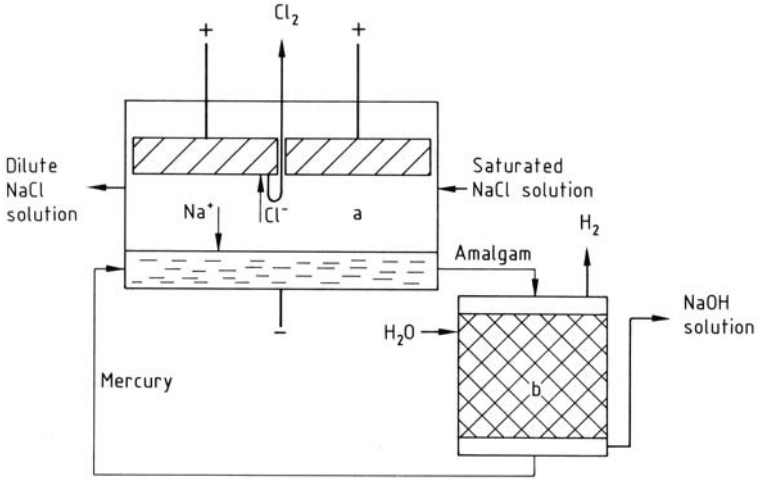

Figure 1. Mercury Process
a) Cell; b) Decomposer

0.3 wt % Na. So high-load mercury cells require large mercury throughputs. Outside the electrolysis cell, the amalgam is treated in a decomposer, a short-circuited galvanic cell. Here the sodium is liberated, and sodium hydroxide solution and hydrogen are formed. The caustic soda solution is both extremely pure and highly concentrated (50 wt %), but the high cell voltage, more than 1 V higher than that required for the competitive processes, and the toxicity of mercury have discouraged use of the highly developed mercury process.

Diaphragm Process. The diaphragm process allows the formation of hydroxyl ions but prevents their movement towards the anode region. The process uses cells divided into compartments by diaphragms made of microporous materials such as asbestos or synthetic polymers. These materials permit the flow of electrolyte but do not allow the OH^- ions to leave the cathode region if there is a sufficient flow of electrolyte from the anode into the cathode chamber, i.e., if the linear velocity of the electrolyte within the diaphragm is somewhat greater than the migration velocity of the OH^- ions in the electric field (Fig. 2 A). This method allows high current efficiencies, but the sodium hydroxide that is formed is contaminated with chloride. The alkali product (50 wt % NaOH) contains 1.3 wt % NaCl, and, hence, further treatment, such as evaporation and crystallization to remove sodium chloride, is unavoidable and expensive, which reduces the economy of the process [2]. And, unless special purification procedures are used, the alkali product (50 wt % NaOH) is contaminated with 1.3 wt % NaCl. The low cell voltage is an advantage, but the electrical resistance of the diaphragm produces an additional potential difference.

Membrane Process. The development of efficient cation-exchange membranes has in general made the diaphragm process obsolete. Fluorinated cation exchange membranes are used. Unlike diaphragms, membranes prevent the hydrodynamic flow of water but permit cation transfer by cation migration, and they enable the almost complete separation of anolyte and catholyte (Fig. 2 B). However, the highly mobile hydroxyl ions cannot be completely prevented from crossing the membrane. High alkali concentration in the cathode region favors OH^- diffusion, contributes to buffering of the anolyte, and promotes hypochlorite formation and its anodic oxidation. The extent of these effects may be gauged by monitoring the oxygen content of the chlorine. As a result, efforts are being made to counteract hydroxide migration by improvements in plant operation, plant design, and membrane quality.

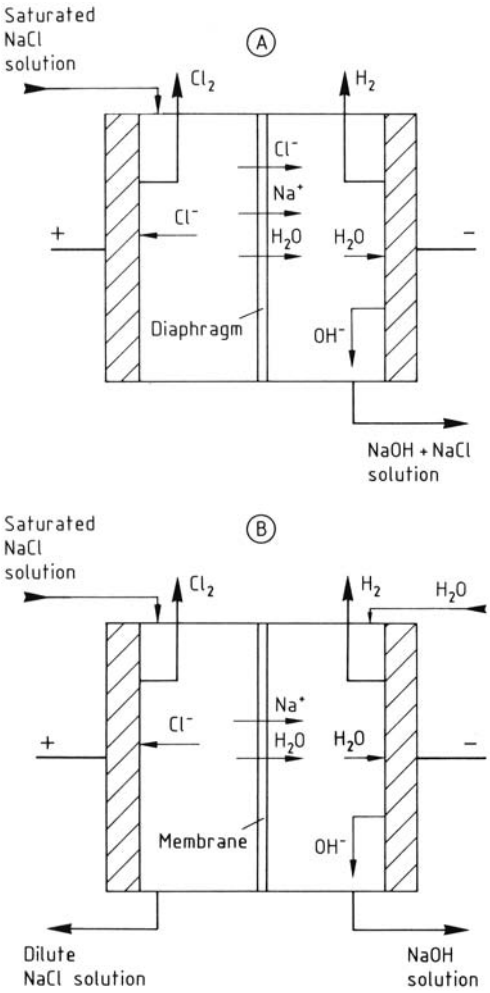

Figure 2. Diaphragm and Membrane Processes
A) Diaphragm cell; B) Membrane cell

The membrane is not completely impermeable to water: the hydrated alkali-metal ion transports a part of its water through the membrane and water arrives at the catholyte side, preventing the concentration of the alkali from attaining the values reached in the mercury process.

Oxygen-Reducing Cathodes. Instead of a hydrogen-evolving electrode, an oxygen-reducing cathode can be used. This alternative allows substantial reduction (ca. 1 V) in cell voltage. Due to its purity, the catholyte of membrane cells is particularly appropriate for the use of air instead of pure oxygen. The high cost of the membranes calls for high current density, ca. 3000 A/m^2, which today cannot yet be met by oxygen-reducing cathodes. The potential cell voltage reduction should stimulate further development [3].

For a detailed description of chlorine production → Chlorine.

1.3. Electrosynthesis of Hypochlorite

In undivided cells hypochlorite is formed instead of chlorine.

$$2\,Cl^- \rightarrow Cl_2 + 2\,e^-$$

$$Cl_2 + H_2O \rightarrow HClO + Cl^- + H^+$$

However, hypochlorite is not a stable product. It is futher converted by anodic oxidation to chlorate or cathodic reduction to chloride. Both reaction rates are mass-transfer controlled. Therefore, high hypochlorite concentrations are impossible to obtain under the conditions for anodic chloride oxidation. The upper concentration limit is ca. 10 g/L. High production rates are possible only if the chloride solution is passed through the cell at high velocity, which also favors mixing of the electrolyte and prevents formation of chlorine gas. But, unfortunately, high electrolyte velocity favors mass transfer of hypochlorite already formed, thus lowering the current efficiency. A through insight into these relationships is a precondition to optimize design and operation of hypochlorite reactor.

1.4. Electrosynthesis of Chlorate

Higher world tonnages are produced by this process than by any other inorganic electrosynthesis. There is no separator between the electrodes in the reactors, and mixing of the electrolyte is an integral feature of the process. The electrolyte, a concentrated sodium chloride solution similar to that used in chlorine production, flows at a high rate through the region between the electrodes. The formation of chlorate, rather than hypochlorite, is encouraged by design and operation of the installation. Chlorate is formed from hypochlorite by two mechanisms, by anodic oxidation

$$3\,ClO^- + 1.5\,H_2O \rightarrow ClO_3^- + 3\,H^+ + 2\,Cl^- + 0.75\,O_2 + 3\,e^-$$

and by partial disproportionation of hypochlorous acid and subsequent autoxidation

$$2\,HClO + ClO^- \rightarrow ClO_3^- + 2\,Cl^- + 2\,H^+$$

This chemical formation of chlorate is the desired reaction in industrial production because, in contrast to anodic oxidation, additional electrical energy is not required.

The anodic oxidation of hypochlorite is mass-transfer limited, and the rate is therefore proportional to the electrode surface and the residence time of electrolyte in the interelectrode gap. The chemical formation, however, is homogeneous, and today all chlorate plants are provided with a comparatively large holding volume in addition to the space between the electrodes, this volume being either integral with the electrolyzer or constructed as a separate unit through which the electrolyte passes. The velocity between the electrodes is high, of the order of 1 m/s. Although this favors the mass transfer of the hypochlorite to the anode, it reduces the residence time in the interelectrode gap. Further conditions favorable to the chemical formation of hypochloric acid are temperatures of 80 – 90 °C, as attainable in modern cells with dimensionally stable anodes, and an optimum pH of 6.1 – 6.4.

1.5. Electrosynthesis of Perchlorate

In perchlorate electrosynthesis, the cell is undivided. Perchlorate is formed solely by anodic oxidation of chlorate. There is, however, a competing reaction, namely the anodic oxidation of water, and this has almost the same standard electrode potential. The relative rate of these two reactions is not significantly affected by pH or other operating conditions. However, the anode potential, which should be high, is of great importance. The process may be optimized only by suitable choice of the material of construction and physical state of the anode. Not surprising then, in contrast to the other process discussed,

there has been no significant recent improvement in perchlorate manufacturing technology.

For a detailed description of hypochlorite, chlorate, and perchlorate production → Chlorine Oxides and Chlorine Oxygen Acids.

1.6. Chlorine Production Using Gas-Diffusion Electrodes [5–7]

In the chlorine production by hydrochloric acid electrolysis a gas-diffusion electrode (GDE) is used as cathode to achieve oxygen reduction and to avoid formation of hydrogen as a byproduct. Hydrochloric acid is a byproduct in various organic processes and its handling and disposal causes serious environmental problems. Electrolysis to supplement the chlorine production produced in alkali cells allows for a viable means to dispose this chemical. Figure 3 schematically shows the design of the cell structure for chlorine production in a membrane cell (see Section 1.3) with a GDE for oxygen reduction, also denoted ODC (oxygen depolarized cathode).

The anode is a common titanium mesh with a catalytic coating of mixed oxides of Ir, Ru, Ti (dimensionally stable anode, DSA). The ODC on the other side of the membrane is in close contact to the Nafion membrane (zero gap technology) and consists of a thin porous reaction layer with an oxygen reduction catalyst and a gas diffusion layer for the distribution of the oxygen and feed of the reaction layer. The scanning electron micrograph in Figure 4 shows a cross-section of the ODC.

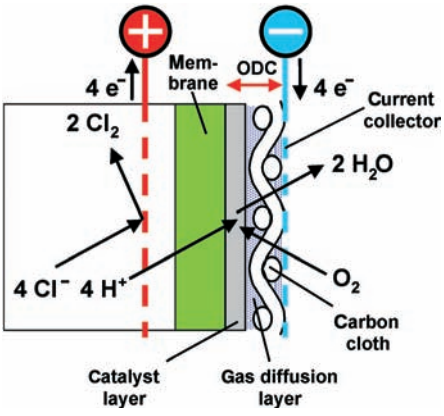

Figure 3. Electrode structure of the membrane cell for hydrochloric acid electrolysis with a gas diffusion electrode as oxygen depolarized cathode

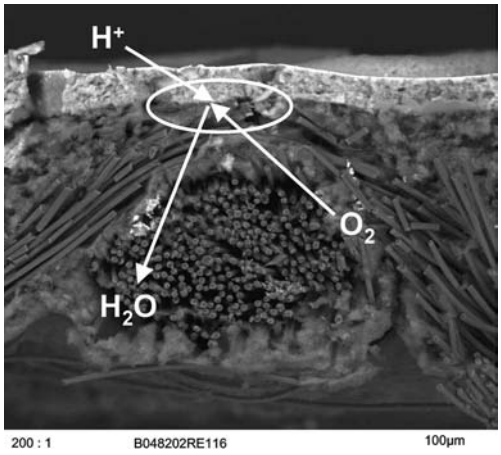

Figure 4. Cross-section of the ODC used in hydrochloric acid electrolysis (scanning electron micrograph)

The reactions involved in hydrochloric acid electrolysis with either hydrogen evolution (Eq. 3) or oxygen reduction (Eq. 2) at the cathode are:

$$4Cl^- \rightarrow 2\,Cl_2 + 4\,e^- \quad \text{at the anode} \quad (E_o = 1.36\,V) \qquad (1)$$

$$O_2 + 4\,H^+ + 4\,e^- \rightarrow 2\,H_2O \quad \text{at the cathode} \quad (E_o = 1.23\,V) \qquad (2)$$

$$4\,H^+ + 4\,e^- \rightarrow 2\,H_2 \quad \text{at the cathode} \quad (E_o = 0\,V) \qquad (3)$$

Replacement of the hydrogen electrode by ODC should lead to a theoretical reduction of the cell voltage by 1.23 V. Practically it is only 1 V, which corresponds to an energy saving of about 50% for the hydrochloric acid process.

Figure 5 shows the cell room of the novel hydrochloric acid electrolyzer developed in a joint cooperation by De Nora Technologie Elettrochimiche, Bayer Materials Science, and Uhde. The electrolyzer consists of a filter press arrangement of planar cells separated from each other by a sheet of ion-exchange membrane. The cell uses hydrochloric acid and oxygen to produce chlorine gas and water. Operating parameters are: 4 kA/m^2, cell voltage 1.3 – 1.5 V, and cell element area 2.5 m^2. The technological changes reduce the energy demand from 1700 kW h per tonne of chlorine to 1100 kW h. The ODC electrolysis may be seen as the forerunner of a new

Figure 5. The modern hydrochloric acid electrolyzer plant for chlorine production installed at Brunsbüttel, Germany (photo Bayer MaterialScience AG)

family of electrochemical processes all based on the GDE technology and characterized by lower energy consumption compared to that of the conventional plants.

The transfer of this technology to the chlor–alkali electrolysis is hampered by the fact that the ODC in this case must work in contact with an aqueous NaOH solution in the cathode compartment. The differences in the arrangements of the two membrane cells for HCl electrolysis and chlor–alkali electrolysis with gas diffusion oxygen reduction cathode GDE are shown in Figures 6a and 6b, respectively.

Operation with a carefully calibrated "finite gap" between the membrane and the oxygen cathode (Fig. 6 B) is necessary to enable the formation of NaOH. The gap is also advantageous, because it allows reutilization of the common periphery after retrofitting from hydrogen to GDE (ODC) operation. A problem is the pressure difference between the electrolyte in the gap and the oxygen gas on the other side of the porous electrode. The electrodes are 1 m or more high, so the hydraulic pressure difference between bottom and top is about 0.1 bar. Without

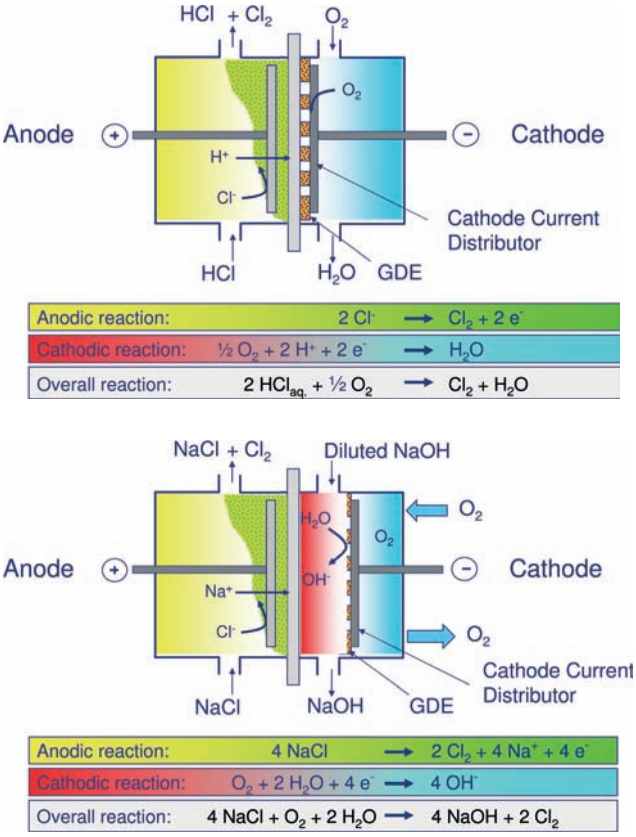

Figure 6. A) HCl electrolysis with gas diffusion electrode for oxygen reduction; B) Chlor–alkali electrolysis with gas diffusion electrode for oxygen reduction

compensation, the pressure gradient $\Delta p = (p_{hydr} - p_{gas})$ may cause flooding of the membrane in the lower part and gas breakthrough in the upper part, which limits the technical application of the ODC. Flooding of the ODC can partly be suppressed by making the membrane hydrophobic. A much better solution is the so called "gas pocket" technology, which was invented by Bayer AG for the chlor– alkali electrolysis using ODCs. The principle is shown in Figure 7. The gas room behind the ODC is segmented by a number of pockets. The gas is pressed into the first pocket at the bottom with a pressure appropriate to the lowest part of the cell. Some gas penetrates the cathode but most escapes and rises as bubbles until it is captured by the blades at the entrance of the second pocket and so on. It is obvious that under these conditions the gas will always have a pressure appropriate to the corresponding depth of the cathode. By this simple self-regulating pressure compensation approach each segment works with an acceptable Δp gradient.

This "gas pocket" technology has been developed at Bayer in cooperation with Uhdenora and is ready for implementation in the chlor–alkali electrolysis end of the 2010s. Its application will be useful for countries where electrical energy is expensive and utilization of hydrogen as a product is not profitable. Another possibility of saving energy without changing the electrolyzer would be the direct conversion of the produced hydrogen to electricity when the fuel cell technology becomes more effective and cheaper.

2. Water Electrolysis for Hydrogen Production

Electrolytic splitting of water [*7732-18-5*] (ΔG^0 = 241.9 kJ/mol, ΔH^0 = 286.66 kJ/mol) corresponds to a decomposition voltage of only 1.2 V and electrical energy consumption per 1 m^3 of H_2 (STP) of only 2.95 kWh, whereas the combustion enthalpy per 1 m^3 of H_2 (STP) of 3.68 kWh corresponds to a "thermoneutral cell voltage" of ca. 1.5 V. In this section, production in m^3 always refers to 1 m^3 of H_2 (STP). The present technology, with cell voltages of $\geq$ 1.9 V and energy consumption of 4.7 – 4.8 kWh/m^3, is still far greater. Water electrolysis is a long-established technique for producing hydrogen [*1333-74-0*] on a commercial scale. Nevertheless, it has gained only limited acceptance for large-scale production. In general, electrical energy, the cost of which constitutes more than half the cost of hydrogen production by water electrolysis, is too expensive to make electrolytic hydrogen competitive with hydrogen obtained by steam reforming of natural gas or oil.

Table 1 presents some information on the few large-scale water electrolysis plants; however, the facilities in Norway are closed now because even there hydroelectricity became too expensive. Nonetheless, the socalled energy crisis of

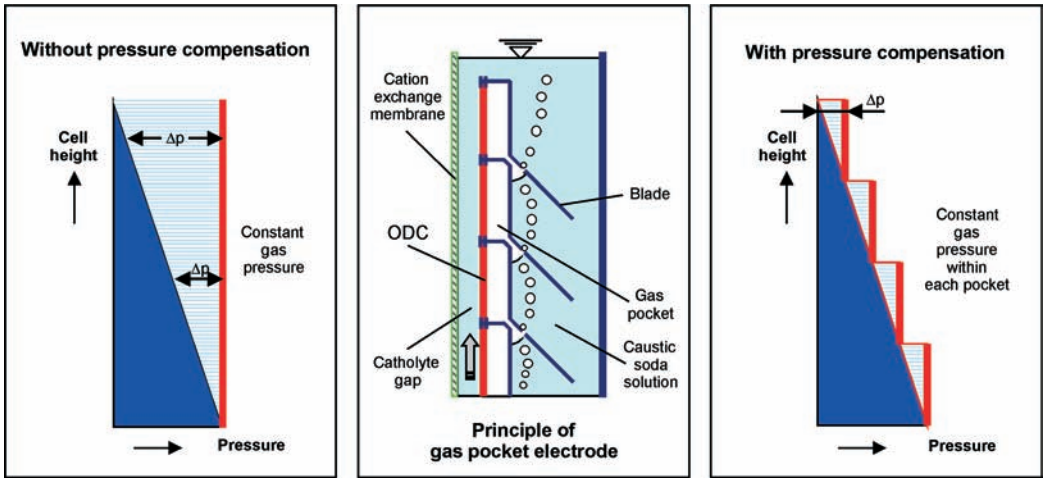

Figure 7. Principle of the "gas pocket" technology for pressure compensation

Table 1. Large-scale water electrolysis plants for H_2 production

Location	Manufacturer	Capacity, m^3 of H_2 at STP
Aswan, Egypt	Brown Bovery	33 000
Nangal, India	De Nora	30 000
Ryukan, Norway	Norsk Hydro	28 000
Ghomfjord, Norway	Norsk Hydro	27 000
Trail, Canada	Electrolyser Inc.	15 200
Cuzco, Peru	Lurgi	4 500

1972, together with potentially more extensive use of nuclear and renewable energies, has led to remarkable efforts to improve the established techniques – in particular alkaline water electrolysis – and to develop new ones – in particular membrane or solid polymer electrolyte (SPE) and high-temperature steam electrolysis.

Hydrogen production is also treated under Hydrogen, 2. Production.

Alkaline Water Electrolysis. With the exception of the Noranda electrolyzer, all electrolyzers of substantial power (> 0.1 MW) currently on the market (Tables 2 and 3) are bipolar electrolyzers with forced convection of the electrolyte. All, with the exception of the newly developed Hydrogen Systems (H. S.) and the MTU electrolyzers, use asbestos diaphragms as separators, and most electrolyzers on the market approach zero-gap geometry.

All electrolyzers are operated with 25 – 35 wt % KOH (with the exception of the H. S. electrolyzer, which uses 14 wt % NaOH), and the process temperature is generally above 75 °C, with an upper limit of 90 °C for the Lurgi and of 130 °C for the MTU electrolyzer.

Most of the electrolyzers work under ambient pressure, leaving compression of the product gases, if necessary, to compressors. Only the Lurgi and MTU electrolyzers, which in some

Table 2. Large-scale commercial ater electrolyzerwater electrolyzers

Characteristic	Manufacturer					
	Electrolyser Corp. (Noranda)	ABB & Cie	Norsk Hydro	De Nora	(Lurgi) Giovanola[*-b]	MTU[**]
Cell type	monopolar tank	bipolar	bipolar	bipolar	bipolar	bipolar
Operating pressure, MPa	ambient	ambient	ambient	ambient	3	3
Operating temperature, °C	70	80	80	80	90	130
Electrolyte	KOH	KOH	KOH	KOH	KOH	KOH
Electrolyte concentration, wt %	28	25	25	29	25	30
Current density, A/m^2	1340	2000	1750	1500	2000	7000 – 10 000
Cell voltage, V	1.90	2.04	1.75	1.85 – 1.95	1.86	1.65 – 1.8
Current efficiency, %	99.9	99.9	98	98.5	98.75	> 99.5
Power consumption (d.c.), kW h per 1 m^3 of H_2 at STP	4.9	4.9	4.1	4.6	4.3	4 – 4.4

[*] Technology transferred from Lurgi to Giovanola s.p.A.
[**] Maschinen und Turbinen Union Friedrichshafen GmbH.

Table 3. Smaller water electrolyzers (100 – 300 m^3/h)

Characteristic	Manufacturer		
	Hydrogen Systems	Hydrotechnik (System Demag)	Krebskosmo
Cell type	bipolar filter press	bipolar filter press	bipolar filter press
Operating pressure, MPa	0.7	ambient	ambient
Operating temperature, °C	120	80	80
Electrolyte	NaOH	KOH	KOH
Electrolyte concentration, wt %	14	25	25
Current density, A/m^2	0 – 5000	1500 – 2500	1000 – 3000
Cell voltage, V	1.5 to 1.7	1.9	1.65 – 1.9
Current efficiency, %	98	99	98.5
Power consumption (d.c.), kW h per 1 m^3 of H_2 at STP	≤3.9	4.9	3.9 – 4.6

ways represent the most ambitious technique, work under medium pressure, 3 MPa, whereas the newly developed H. S. electrolyzer operates at an only moderately enhanced pressure of 0.7 MPa. Low-temperature operation (< 80 °C) under ambient pressure permits the use of light equipment such as normal steel for electrodes, cells, pipes, pumps, etc., and helps keep investment costs low. Higher temperature and pressure call for heavier construction and for more care in particular to selection of steels with reliable corrosion stability and insensitivity towards stress corrosion cracking.

The advantages of higher temperatures and pressures are, however, convincing with respect to power consumption. Higher temperatures reduce the cell resistance because of improved electrolyte conductivity and reduce the electrode overpotentials due to thermal activation of the electrode process. High pressure reduces the volume of the evolved gases and gas holdup in the cell and thus reduces the effective electric resistance of electrolyte.

→ Electrochemistry, 1. Fundamentals, Figure 13 depicts a cell voltage – current density curve that is typical for the present electrolyzer generation having effective surface specific resistance around 1 Ω cm^2. For improved pressurized electrolyzers this resistance is some 70 to 80 % less (Fig. 8). The steep increase of cell voltage with current density – mainly due to the relatively high cell resistance – is a good reason to keep current densities in conventional electrolyzers low, 0.2 – 0.3 A/cm^2, thus conserving

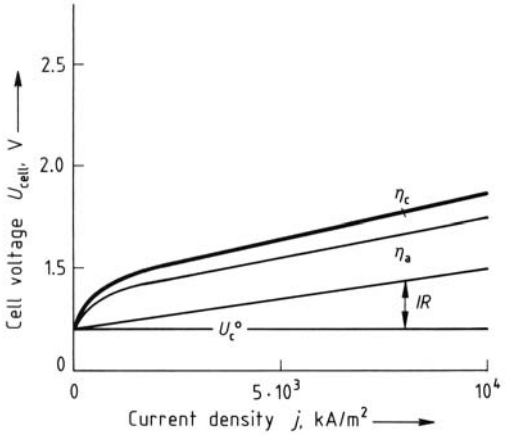

Figure 8. Current – voltage curves for advanced alkaline water electrolysis [4]

expensive electrical energy. Only the Lurgi electrolyzer in its most modern version, the MTU and the H. S. electrolyzers aim at current densities upwards of 0.5 A/cm^2 and can do so because of their relatively low surface specific resistances.

The three most advanced electrolyzer technologies allow hydrogen production with an energy consumption of 3.8 kWh/m^3 at current densities as high as 0.8 A/cm^2. This energy consumption approaches the water-splitting enthalpy of 3.68 kWh/m^3.

Electrocatalysis. Relatively little effort is needed to catalyze the cathode reaction. Most commonly used are high surface area nickel layers, either Raney nickel [*7440-02-0*] or porous nickel coatings produced in situ by cathodic reduction of nickel sulfide coatings.

$$Ni_2S_3 + 6\,e^- \rightarrow 2\,Ni + 3\,S^{2-}$$

Leachable Ni_2S_3 coatings are obtained either by cathodic nickel deposition from galvanic Ni^{2+} baths containing sulfur donors (thiosulfate, thiourea, thiocyanate, and similar compounds) or by sulfidizing nickel electrodes in an atmosphere containing hydrogen sulfide. Raney nickel coatings can be applied on steel or nickel electrodes by cold-rolling [8]: the Raney nickel (Ni – Al prealloy containing 50 wt % Ni, corresponding approximately to stoichiometry $NiAl_3$) is bonded by pressure and shear to the electrode and is stabilized by subsequent annealing on the electrode. A second method consists of cathodically depositing Ni – Zn alloys containing Ni : Zn ratios in the range 1 : 1 to 2 : 1 [9]. Such coatings are relatively thin, between 50 and 150 μm. The well-established theory of porous electrodes indicates that the penetration depth of the current in these highly porous electrocatalysts is ca. 100 μm for current densities around 1 A/cm^2.

Improvements for advanced electrolyzers aim at decreasing cell resistances, the objective being to increase current densities above 0.5 A/cm^2 and still decrease cell voltages below the values used in the established technology. Electrocatalysis, especially at the anode, is now being introduced for the established electrolyzers as well.

Prior to public disclosure of the results of the recent research and development almost the only anodic electrocatalyst was nickel or nickel-coated steel anodes. NiO, or rather NiOOH, is by itself – compared to other metal oxides – a

relatively effective electrocatalyst to enhance anodic oxygen evolution, and allows the use of an anodic overpotential lower than + 280 mV at current densities of 0.1 – 0.2 A/cm^2 at 90 °C in 30 wt % KOH.

Coatings of mixed oxides containing cobalt oxide such as cobalt nickel calcium perovskite and lanthanum nickelate ($Ca_{0.2}Co_{0.8}LaO_3$ – $NiLaO_3$), cobalt nickel spinel (Ni_2CoO_4), and cobalt spinel (Co_3O_4), and iron – cobalt mixed spinel have proved to be relatively efficient electrocatalysts for anodic oxygen evolution. Indeed, the new H. S. electrolyzer is known to use Co_3O_4 coatings at the anode.

Diaphragms. Most impressive are the advances made in replacing the thick asbestos diaphragm – its thickness causing excessive electrolyzer resistances – by much thinner, mechanically strong diaphragm structures with electrical resistances approximately one order of magnitude lower than those of asbestos diaphragms.

The new separators make use of composite materials because one material seldom is able to fulfill the many opposing demands simultaneously – for instance, high porosity small thickness, and high mechanical strength. The diaphragm of the H. S. electrolyzer, for instance, is based on polysulfone, a mechanically strong, relatively easily processed, but hydrophobic polymer. In the form of highly porous sheets it is hydrophilized internally by finely dispersed zirconia, an inorganic oxide of low water solubility. Similarly, porous PTFE sheets can also be hydrophilized by dispersed zirconia.

Quite different and comparably successful is the approach of using nickel net-supported porous ceramics such as NiO or $CaTiO_3$– Ni cermets, yielding mechanically stronger and more robust, yet flexible, diaphragms.

Water Electrolysis with Cation Exchange Membranes (SPE Electrolysis). The aqueous electrolyte may be completely dispensed with by use of a sheet made of proton-loaded water-swollen cation-exchange polymer as electrolyte (the solid polymer electrolyte, SPE, Fig. 9 A, also see Fig. 32), which was first introduced by General Electric for fuel cells in space missions (Gemini flights). This fuel-cell option has successfully been converted into electrolyzer technology and offers a promising solution for small

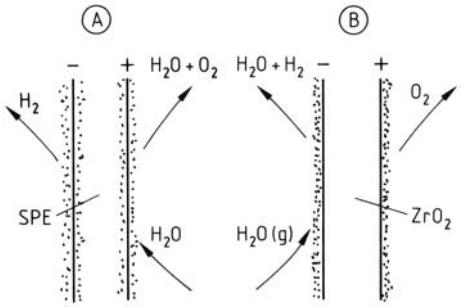

Figure 9. Nonconventional electrolyzers
A) Solid polymer electrolyte (SPE) electrolyzers decomposing deionized water at ca. 100 °C; B) Steam electrolyzers with zirconia electrolyte decomposing water vapor at 800 – 900 °C

electrolyzers: any dangers and difficulties involved in handling hot concentrated caustic alkali solutions are avoided.

The electrodes are formed within the outer layers of Nafion membranes by interdiffusing two solutions, one containing salts of the platinum group metals, the other an appropriate reducing agent, and precipitating in situ a coherent highly porous catalyst layer on either side of the membrane. The primary electrode deposits are then reinforced by further metal deposition. Current is transmitted through porous plates (platinized titanium anodes and carbon cathodes) and dense bipolar metal sheets. The porous metal plates permit simultaneous feeding of the highly purified water to be decomposed and removal of the evolved gases. Fig. 10 compares the current voltage curve for the solid polymer electrolyte electrolyzer with that of advanced alkaline electrolyzers and the steam electrolyzer. Typically, SPE elec-

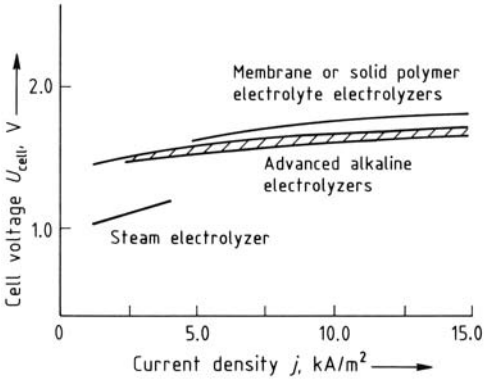

Figure 10. Comparison of current – voltage curves of solid polymer electrolyte, advanced alkaline, and steam electrolyzers

trolyzers are operated at current densities around 1 A/cm^2. At lower current densities, current efficiencies decrease substantially below 100 % because of counterdiffusion of the generated gases through the < 50-μm ion-exchange membrane.

High-temperature Steam Electrolysis. The ionic conductivity of zirconia, which between 800 and 900 °C becomes comparable to that of 10^{-1} M aqueous electrolyte solutions at ambient temperature, permits high-temperature steam electrolysis. This technique is particularly appealing because the decomposition voltage, as calculated from ΔG°, decreases as the temperature increases and drops to a value of only 0.9 V around 850 °C. The cell scheme (Fig. 9 B) resembles the SPE cell. The cathodes are made of nickel cermet and the anodes consist of semiconducting Mn-containing perovskite layers. Although much effort has gone into the development of this electrolyzer, which is realized in the form of small cylindrical elements of 1 cm × 1 cm size, the technique is still far from competitive with conventional or advanced alkaline water electrolysis. The operating cell voltage of 1.3 – 1.4 V is still far from the theoretical 0.9 V, and quite a number of material problems are also unsolved. In particular, the thickness of the electrolyte is still too high, so that the internal resistance of the cell does not permit current densities of more than a few hundred milliamperes per square centimeter. It might be possible that the development of solid oxide fuel cells leads to substantial improvements of steam electrolysis. At present, SPE and steam electrolysis are not commercially available.

3. Anodic Generation of Peroxodisulfuric Acid and Peroxodisulfates

Peroxodisulfuric acid and its salts – in contrast to the salts of most other inorganic peroxo acids, which are prepared chemically – are produced exclusively by anodic oxidation of aqueous sulfuric acid solutions:

$$2\,SO_4^{2-} \rightarrow S_2O_8^{2-} + 2\,e^-$$

Preconditions for attaining high current yields in this process are the use of high concentrations of sulfuric acid (ca. 500 g H_2SO_4 per liter), high current densities (0.5 – 0.7 A/cm^2), low process temperature (18 – 20 °C), the addition of O_2-evolution inhibitors such as F^- anions, and the use of smooth platinum anodes, which favor adsorption of SO_4^{2-} anions. Reduction of the product is prevented by porous coatings on the cathode, which build up a diffusion barrier for peroxodisulfate anions.

Potassium, sodium, and ammonium peroxodisulfates are prepared with similar electrolysis technology from solution of the alkali-metal or ammonium sulfates and sulfuric acid (→ Peroxo Compounds, Inorganic).

4. Electrowinning and Electrorefining of Metals

4.1. Aqueous Electrolytes

Pyrometallurgical winning of metals is less expensive by far than electrowinning of metals by cathodic deposition from aqueous solution. But the pyrometallurgical processes have slight or only partial purification effects and yield impure metals that do not satisfy quality standards. Therefore, electrowinning and electrorefining have become important for the production of high-quality copper, zinc, lead, nickel, and cobalt. Electrorefining is based on the potential series of metals [10]. Anodic dissolution of impure metals if the current densities are small and therefore the overpotential negligible leaves the noble components of raw, unrefined metals undissolved. These noble components precipitate in the so-called anode slime or sludge, whereas the metals that are less noble than the metal being electrorefined dissolve with the main metal but are not redeposited on the cathode. Therefore, the less noble metals accumulate in the aqueous electrolyte. For any two metals M_1 with standard electrode potential E_1^0 and M_2 with E_2^0, the voltage difference $(E_1^0 - E_2^0)$ establishes the anodic dissolution equilibrium and defines the concentrations c_1 and c_2 of the two metal ions in equilibrium at a given electrode potential E according to the Nernst equation

$$E = E_1^0 + (RT/z_1F)\ln c_1 = E_2^0 + (RT/z_2F)\ln c_2$$

$$\frac{(c_1)^{1/z_1}}{(c_2)^{1/z_2}} = \left\{\exp -\frac{F(E_1^0 - E_2^0)}{RT}\right\}$$

The second equation neglects the activity coefficients of the metals and is applicable only if electrochemical dissolution/deposition is a fast process for both metals. This is the case for the metals Cu, Zn, and Pb but not for Ni, Co, and Fe. The deposition/dissolution of nickel is particularly sluggish, which diminishes the efficiency of an electrorefining process involving nickel because enhanced overpotentials are generated at both the anode and the cathode.

Alloy formation, which may change the chemical activity of the minor components greatly, is also not allowed for in the equation. For instance, zinc alloyed in nickel ultimately codeposits with nickel, although according to the difference in standard electrode potentials, $E^0_{Ni} - E^0_{Zn} = 0.53V$, the equilibrium concentration of the two ions should differ by a factor of 10^9. However, zinc becomes much more noble upon alloying.

Such effects and the accumulation of impurities in the recirculated electrolyte make chemical treatment and purification of the electrolyte indispensable for all electrowinning and electrorefining processes. Since electrowinning with insoluble anodes starts from cruder materials than electrorefining, the chemical purification of the electrolyte must be even more elaborate and expensive for electrowinning than for electrorefining.

Therefore, the important purification steps for electrowinning of nonnoble metals, like zinc, are hydrometallurgical rather than electrochemical. This is exemplified by the flow sheet in Fig. 11. The process begins with roasted galena, which is leached with recirculated electrolyte (cell acid). The silver and lead remain in the sludge. All elements nobler than zinc are then precipitated by cementation with zinc dust, and the cemented sludge is treated further to recover Cd, Ni, Co, and Fe. Iron can disturb zinc electrowinning seriously by electrochemical short circuiting:

Cathode $Fe^{3+} + e^- \rightarrow Fe^{2+}$

Anode $Fe^{2+} \rightarrow Fe^{3+} + e^-$

Therefore, iron(III) ions are precipitated as jarosite, a crystalline iron(III) sulfate oxide hydrate of extremely low solubility. As a second example, in copper refining accumulated nickel and other contaminants must be removed in a bleed stream.

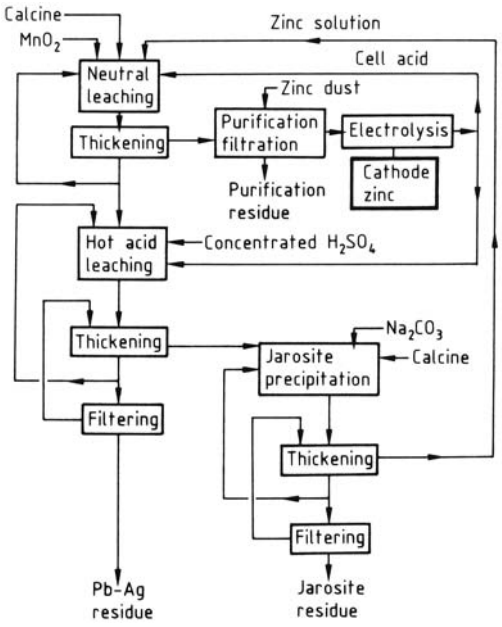

Figure 11. Flow sheet of the jarosite process [11]

For electrowinning and electrorefining of metals, mass transfer towards the cathode is of supreme importance. Convective diffusion driven by free (only gravity) convection caused by depletion of the solution at the cathode dominates mass transfer in these electrolysis processes. Anodes and cathodes, typically 0.8×1.2 m^2, are suspended vertically at a distance around 10 cm from each other. They are arranged alternately one after the other in large rectangular tanks, which contain several hundred electrodes. Although there is a steady flow of electrolyte from one end of these huge tanks to the other, the flow velocity is small and electrolyte flow is not directed parallel to the electrode surface and thus does not contribute to convective mass transfer towards the electrodes to a significant degree.

The electrolyte for copper electrorefining contains ca. 40 g of Cu per liter (a concentration somewhat less than 1 M) and total depletion of copper from the solution decreases the density by several grams per 100 mL, i.e., by several percent. The Grashof number under these conditions

$$Gr = (x^3\, g\, \Delta\varrho/\varrho)/\nu^2$$

would exceed the critical value of 10^{15} for x, the distance from the lower edge of the cathode, where the electrolyte is depleted of Cu^{2+} ions

by electrodeposition of copper for turbulence; this distance x exceeds several centimeters. Therefore, for the greater part of the cathode length, usually of the order of 1 m, turbulent flow, with correspondingly intense mass transfer, prevails. But since mean mass-transfer coefficients do not exceed ca. 10^{-3} cm/s, mean current densities for cathodic metal deposition in electrowinning and electrorefining processes must be kept low, on the order of 200 mA/cm^2, to stay well below mass-transfer-limited current densities. Higher current densities cause the quality of the deposited metal to deteriorate: the deposit becomes coarse, forms whiskers, and begins to occlude or incorporate electrolyte, floating anode slime, and other impurities.

Even at current densities significantly lower than mass-transfer-limited values, deposit quality must be improved with surfactants. These additives increase the crystallization overpotentials for the deposited metal – inducing frequent nucleation, which gives rise to smooth cathode surfaces with little inclusion of foreign substances. Such surfactants are absolutely necessary for obtaining highly purified metals and preventing the formation of dendrites, which can short-circuit the cell. Cheap, widely used additives are animal glue (gelatin), lignin sulfonates, and aloe extract, the last mainly polyphenols. All these additives are continuously consumed because of hydrolysis, oxidation by air, and adsorptive incorporation into the deposited metal and the anode slime.

Anodes for electrowinning processes are conventionally made of lead with few percent of silver. They have remarkably high oxygen-evolution overpotentials. In the future, activated titanium anodes will become more important.

Unlike all other electrochemical and chemical processes, the cost factor labor is extraordinarily high for electrowinning and electrorefining of metals because of the frequent electrode handling. In a process with anode lives of ca. 30 days (Cu, Ni) or only 10 – 14 days (Pb), and even shorter life spans for cathodes, there is the constant necessity of anode casting and the exchange of anodes and cathodes. Continuous progress in automatization is vital for the survival of these processes.

Aside from the labor costs, the cost structure of these processes are unique because of the investment costs for solution processing and the electrolyzer tank house and the capital required for the metal inventory in electrodes and circulated electrolytes.

Copper Electrowinning and Electrorefining. Copper [*7440-50-8*] is almost always electrorefined, less frequently electrowon. The raw material is the raw copper obtained by reduction of the oxidic ores or concentrates with carbon in a blast furnace. Raw copper is cast into anodes containing roughly 98 % Cu, the rest being mainly nickel and lead, with a fraction of a percent of noble metals, especially silver.

Table 4 summarizes the operational conditions. Nickel sulfate removal is accomplished in a bleed stream from which copper is electrowon prior to evaporation and crystallization of $NiSO_4$. The removal of Cu in *liberator cells* serves to balance the copper content of the bath and offset the additional chemical dissolution of copper due

Table 4. Typical energy requirements in electrorefining and electrowinning

	Copper		Nickel refining		Zinc electrowinning
	Refining	Winning	Metal anode	Sulfide anode	
Current density, mA/cm^2	210	300	200	200	570
Current efficiency, %	97	85	96	96	90
Cell voltage, mV	280	2000	1900	3700	3500
Reversible cell voltage	0	900	0	350	2000
Cathodic overpotential	80	50	250	1500	150
Anodic overpotential	30	600	300	250	600
Ohmic voltage drops	100	400	1050*	1250*	500
Cell hardware IR	70	500	300	350	250
Electric energy requirement, kW h/kg	0.25	2	1.9	3.5	3.3

* With diaphragm.

to oxidation by dissolved oxygen, which otherwise tends to increase the Cu^{2+} content of the electrolyte steadily (→ Copper, Section 6.2).

The cost contribution of electrical energy is an insignificant fraction of the whole process cost. Therefore, increasing the space – time yield is of special concern. Increasing the current density by at least 50 % by periodic current reversal is one approach now being used. The current is reversed for 10 s out of every 200 s, and correspondingly 5 % of the deposited copper is redissolved. This causes electropolishing, which produces high-quality, smooth deposits at high current densities. Another approach (Onahama refinery, Japan) consists of casting thinner anodes, which reduces the copper inventory by 50 %, and increases the space – time yield by ca. 20 % because the electrodes can be spaced closer together without short-circuiting. However, labor costs are increased by this measure, as does the amount of recycled anode scrap.

Electrowinning of copper is not fundamentally different from electrorefining, except that the depleted electrolyte is recirculated to leach copper ores. Purification is today mainly based on solvent extraction. The current densities can be greater for electrowinning because the stirring by the oxygen evolved at the anode enhances bath convection and mass transfer.

For more details see→ Copper.

Nickel Electrowinning. Nickel [*7440-02-0*] electrowinning begins with either crude nickel or nickel matte (Ni_2S_3) anodes [11, p. 357 ff]. In both cases the metallic contaminants to be removed are the same: mainly copper, cobalt, and iron. In both cases the anolyte must not be allowed to enter the cathode chamber prior to purification. In the Hybinette cell (Fig. 12), the cathodes are surrounded by a cathode bag. The depleted catholyte flows out of the cathode bag into the anode chamber because of a small hydrostatic head. In the anode chamber, nickel ions pass into the electrolyte:

$$Ni \rightarrow Ni^{2+} + 2\,e^-$$

or

$$Ni_2S_3 \rightarrow 2\,Ni^{2+} + 3\,S + 4\,e^-$$

Then the recycled electrolyte is purified. Copper(II) is extracted by cementation with nickel powder, and iron and cobalt are precipitated together with lead by oxidation with chlorine and addition of basic $NiCO_3$. If nickel matte is the starting material, purified sulfur is recovered from the anode sludge. The operational conditions for both processes are shown in Table 4. Starting from nickel matte, rather than raw nickel, requires higher cell voltages, much higher than would be expected from the difference between the two standard electrode potentials, which differ by only ca. 0.3 V. This much higher cell voltage is caused by electrode kinetic hindrance and additional ohmic potential drop on account of an adherent porous layer of sulfur that covers the anode.

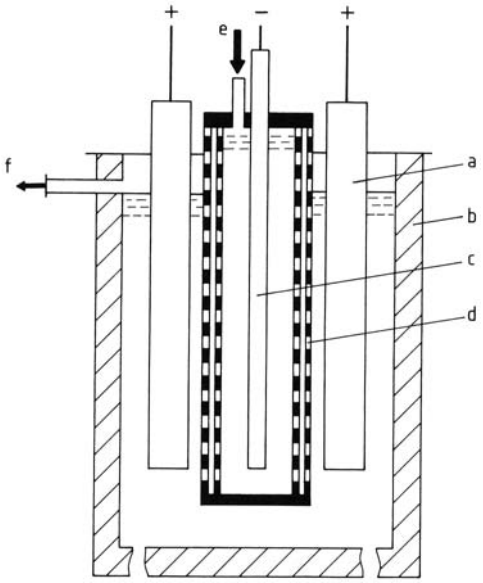

Figure 12. Hybinette cell for nickel electrowinning [11, 12]
a) Anode; b) Cell wall; c) Cathode; d) Diaphragm; e) Catholyte inlet; f) Anolyte exit

For more details see → Nickel.

Zinc Electrowinning. The chemical purification procedures involved in electrowinning zinc [*7440-66-6*] were discussed, as an example, at the beginning of this section. The peculiar circumstance of zinc electrowinning is the negative standard electrode potential of zinc (− 0.76 V), which would make zinc deposition impossible except for the fact that hydrogen evolution at zinc cathodes has a very high overpotential ($j_0 = 10^{-11}$ A/cm^2). Nevertheless, care must be taken to keep the current efficiency for zinc

deposition as high as ca. 90 %. The process is carried out at the rather low temperature of 35 °C. Ten percent of the current goes into hydrogen evolution, which improves mass transfer enough that current densities can exceed 0.5 A/cm^2. The operational conditions for zinc electrowinning are listed in Table 4 [11, p. 363 ff].

For more details see → Zinc.

Lead Electrorefining. The electrorefining of lead [*7439-92-1*], introduced in 1903 as the Betts process, is especially effective in separating bismuth, which goes into the anode sludge. Chemical treatment of bullion is used to remove copper, and subsequently tin (together with As, Sb, and Bi) by precipitation with caustic soda. The crude anodes consist of (wt %) ca. 98 % Pb, 0.5 % Bi, 0.01 % As, 1 % Sb, 0.02 % Cu, and 0.02 % Sn. The electrorefining process uses either hexafluorosilicic acid (H_2SiF_6) or sulfamic acid (HSO_3NH_2) as the electrolyte. Current densities are somewhat higher for the processes working with H_2SiF_6 (160 – 200 mA/cm^2) than for the sulfamic acid process (120 – 160 mA/cm^2). In both cases a relatively low temperature is maintained to retard hydrolysis of the electrolyte [11, p. 356 ff].

For more details see → Lead.

4.2. Melts

Manganese ($E^0 = -1.05$ V) is the most reactive metal that can be electrodeposited from aqueous solution. Metals even more reactive – aluminum, magnesium, and the lanthanides – are electrodeposited from salt melts. Cathodic hydrogen evolution, due to water decomposition, cannot interfere with cathodic metal deposition. Normally melt electrolysis is not used as a purification step because of the difficulty of purifying and recycling contaminated melts. A thoroughly purified oxide is the starting material for electrowinning. The Bayer process, for instance, is an integrated step in aluminum production since it produces aluminum oxide of very high purity (impurities < 0.1 wt %) from crude bauxite. The Bayer process is responsible for 40 – 50 % of the production cost of aluminum [13, p. 296].

Typical problems posed by melt electrolysis are first of all material problems: the *stability* of (1) cell linings against chemical attack of the usually agressive melt, (2) anodes against the corrosiveness of the anode gases (Cl_2, O_2), and (3) cathode material against reaction with the liquid metal. These three problems are especially severe because of the high process temperature, usually above the melting point of the metal: 660 °C (Al), 648 °C (Mg), and 97 °C (Na).

A second typical problem is dispersion or dissolution of the liquid metal into the electrolyte, which allows partial reoxidation due to convective transport of the metal mists toward the anode. There the metal reacts with evolved gas, or it is directly reoxidized at the anode. This phenomenon is caused by (1) the low surface tension of molten metals in contact with the molten electrolyte, (2) the relatively small density differences between molten metal and molten salt, and (3) strong convection due to magnetohydrodynamic effects and gas stirring. Cell geometry must be designed to suppress excessive convection or to provide a sufficiently large interelectrode gap (ca. 8 cm in aluminum smelters) to minimize metal reoxidation.

A further engineering aspect that is unique and typical for all high-temperature electrolytic processes is the careful calculation of heat balances and heat isolation devices for electrolyzers and potlines, which is indispensable for energy conservation and for steady, reliable operation of molten-salt electrolyzers over months and years.

Aluminum Production [13–15]. The electrolytic production of aluminum [*7429-90-5*] by electrolysis of Al_2O_3 dissolved in cryolite (Hall–Héroult process) is by far the most important electrochemical process based on the use of a molten-salt electrolyte.

$$Al_2O_3 + 3\,C \xrightarrow{6F} 2\,Al + 3\,CO$$

Six faradays of electricity are required for each mole of Al_2O_3.

The addition of Al_2O_3 to cryolite (*mp* ca. 1000 °C) decreases the melting point as the alumina content is increased up to 10 wt %, where the eutectic melts at 960 °C [15].

Figure 13 depicts the construction of a modern Hall–Héroult cell schematically. The cell is composed of an outer carbon or graphite lining and a row of adjustable prebaked carbon anodes. At the bottom of the pot there is the cathode, a pool of liquid aluminum, which is emptied

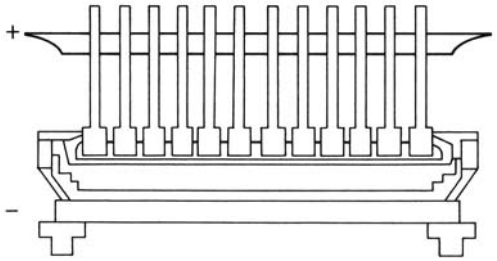

Figure 13. Hall – Héroult cell

periodically by suction and which is covered by the molten electrolyte into which are immersed the gas-evolving anodes. The melt is covered by a crust of solid electrolyte and a supply of fresh, loose Al_2O_3. Periodically crushing this crust serves to replenish the Al_2O_3 content of the bath. The cathodic reaction consists of reducing fluoro-oxo-aluminum complexes:

$$AlOF_n^{(n-1)-} + 3\ e^- \rightarrow Al + O^{2-} + nF^-$$

A mixture of carbon monoxide and carbon dioxide is evolved at the anode: the depolarizing carbonaceous anode material reacts with the anodically generated oxygen,

$$(x+y)C + (x+2y)O^{2-} \rightarrow x\,CO + y\,CO_2 + (2x+4y)e^-$$

In accord with this anode reaction, the Hall – Héroult process consumes significant amounts of extra energy due to the consumption of the carbon anode.

There is violent stirring of the molten metal and the electrolyte due to magnetohydrodynamic effects and anodic gas evolution. Vigorous stirring may cause severe losses in current yields and energy efficiency. The reoxidation of metal mists at the anode or the reoxidation of the dispersed metal by the anode gases causes a loss of energy. These energy losses are avoided to a certain extent by increasing the anode – cathode distance. Aluminum smelters operated with optimal interelectrode distances of a little less than 8 cm achieve current efficiencies exceeding 93 % and electrical energy consumptions of optimally 13 kW h/kg (theory: 6.34 kW h/kg). The relatively low energy efficiency of the Hall–Héroult process is the reason more energy-efficient electrolysis processes have been sought.

In 1954, Alcoa resumed the work of BUNSEN [16], who was the first to produce aluminum metal by electrolysis of alkali chloride – aluminum chloride melts. Alcoa developed the technology of aluminum deposition from alkali chloride – aluminum chloride melts up to a commercial scale. The Alcoa electrolyzer uses stacks of bipolar carbon electrodes. The upper parts serve as cathodes, and the lower grooved parts serve as chlorineevolving anodes. This electrolyzer is reported to produce aluminum metal with a specific energy demand of 10 kW h/kg, offering a 30 % saving in electrical energy over the Hall–Héroult process. In LiCl melts of low $AlCl_3$ content the energy savings seem to be still more promising [17]. However, further development of chloride electrolysis technology also requires the development of a commercially attractive route for $AlCl_3$ production from bauxite [17]. However, the Alcoa process eventually failed, because the anodically generated chlorine was contaminated with perchlorinated aromatic compounds which could not be eliminated at reasonable costs.

For more details on aluminum production, especially the Hall–Héroult process, see → Aluminum.

Magnesium and Alkali Metal Production. Figure 14 shows the decomposition potentials of the alkali-metal chlorides as functions of temperature. Magnesium chloride, with a decomposition voltage of 2.6 V at 700 °C is the most easily decomposed chloride among the Group 1 and 2 chlorides.

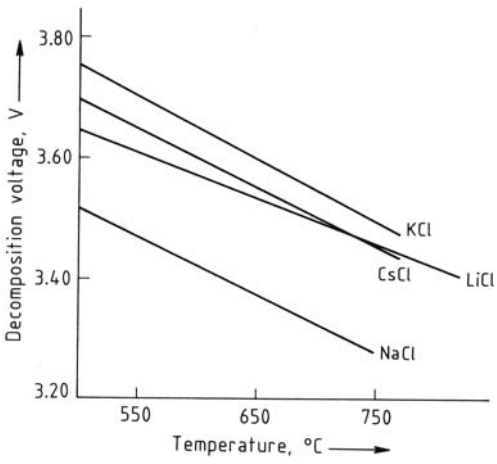

Figure 14. The decomposition potentials of the alkali-metal chlorides as functions of temperature [18]

Table 5. Working temperatures, cell voltages, and current efficiencies in the production of light alkali metals and alkaline-earth metals

Cell operating characteristics	Metal		
	Lithium	Sodium	Magnesium
Working temperature, °C	400 – 420	590 – 600	660 – 670
Cell voltage, V	8 – 9	6.5 – 7	5.5 – 6
Current efficiency, %	85 – 90	90 – 95	78 – 80

The light alkali metals and alkaline-earth metals magnesium, lithium, sodium, and potassium have lower densities than the melts of their chlorides. Therefore, the electrodeposited metals ascend through and collect on top of the chloride melts. They must be prevented from coming into contact with the electrogenerated chlorine.

Interelectrodic gaps of several centimeters together with steel diaphragms between the electrodes and steel collectors that gather the ascending metal droplets above the cathode allow effective separation of chlorine and liquid metal – but at the expense of relatively high cell voltages and relatively low energy efficiencies. Nevertheless, metal dispersion and the solubility of metal in the melt are reasons for low current efficiency (Table 5). The trade-off between high current efficiency and low cell voltage results in energy yields between 30 % and 40 %, which are typical for salt-melt electrolysis but which are low compared to large-scale electrolysis processes with aqueous solutions.

For more details see → Lithium and Lithium Compounds, → Magnesium, → Potassium and Potassium Alloys, and → Sodium and Sodium Alloys.

5. Electrochemical Processes in Nuclear Fuel Reprocessing

Oxide fuel light water reactors (LWR) are dominant for nuclear electricity production worldwide. For this type of fuel an aqueous medium process to recover the fissionable material is well established. The zirconium alloy-clad fuel elements containing uranium oxide – plutonium oxide fuel are cut up, and the uranium and plutonium are leached out of the cladding material with nitric acid. Afterwards the solution is purified by multiple extractions using *n*-tributyl-phosphate (TBP) diluted with kerosene (→ Nuclear Technology, 3. Fuel Cycle, Section 4.1). This process, the Purex process, was first developed in the late 1940s and industrially used in the USA in the early 1950s.

Determined by the demand of the following processes for reenrichment and fuel fabrication to minimize shielding and to facilitate the handling of the refabricated fuel elements, it is a particular requirement for the reprocessing process to guarantee an extreme product purity and to keep the contents of radioactive contaminants as low as possible. The permissible contamination limit for the long lived fission product cesium, after reprocessing, is, for example, about 3 μg/kg and the residual content for plutonium is limited to about 15 μg/kg in the uranium product. Furthermore, the process calls for a high product yield of 99 %. For the extraction process about 99.5 % is achievable in a modern plant. On average, this corresponds to a content of about 1 mg/kg plutonium in the extraction raffinates.

Another requirement of commercial reprocessing is minimization of the radioactive waste volume in order to reduce costs. The costs of radioactive waste treatment and storage are incomparably higher than the actual costs for conventional chemical wastes. The major part, more than 50 % of reprocessing costs are capital costs. This is the reason why current R&D activities are directed to a cost reduction by a simplification of the process.

Figure 15 shows a schematic diagram of the Purex process (see also → Nuclear Technology, 3. Fuel Cycle, Section 4.1.7). Five extraction cycles are used to meet the product specifications. In the first high-active cycle the major portion of fission products is separated from uranium and plutonium. A radioactivity portion of about 10^{-5} of the 'nonproblematic' fission products and actinides (alkali, alkaline-earth, rare earth, transplutonium elements, etc.) leave this cycle with the products uranium and plutonium. The products are separated later by reducing tetravalent plutonium to Pu(III) which has a very low distribution coefficient and is backextracted into an aqueous phase. Between each cycle plutonium has to be reoxidized and hydrazine, which is necessary to stabilize plutonium in the trivalent state, must be destroyed by oxidation.

One reason for incomplete separation is the degradation of the solvent by radiolysis and

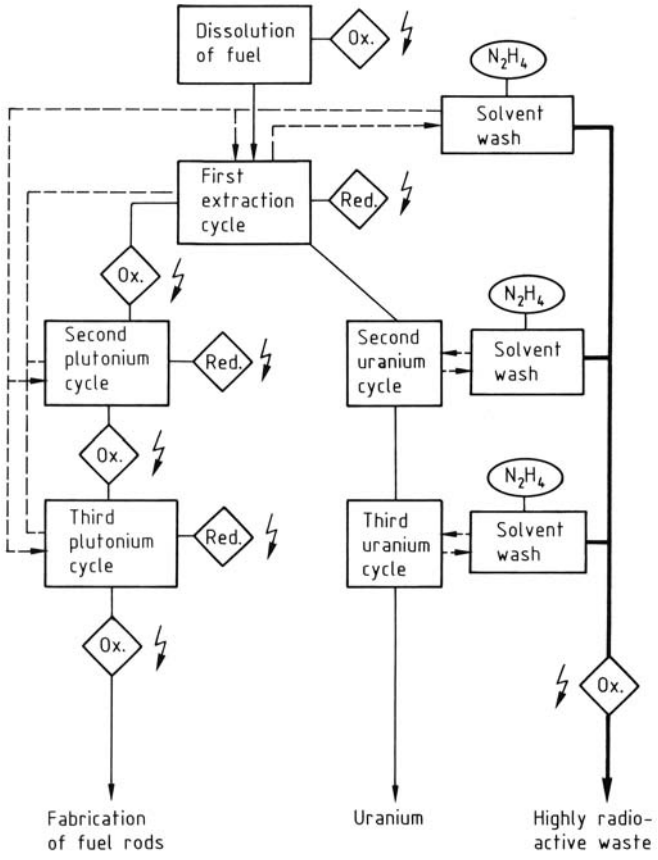

Figure 15. Schematic diagram of the PUREX process
The jagged arrow indicates an electrochemical process

hydrolysis [19]. Some fission products and plutonium form complexes with the TBP degradation products. Thus the degradation products must be removed by an alkaline wash.

Both laboratory and industrial experiences with the conventionally designed high-active first Purex cycle show that the product purity specifications cannot be met, even for the 'nonproblematic' fission products [20]. Therefore, two additional refining cycles are used for each product, uranium and plutonium (see Fig. 15).

5.1. Electroredox Separation Processes

In order to separate uranium from plutonium, Pu (IV) is reduced to virtually inextractable Pu(III). For the reduction of plutonium, four processes have been developed to technical maturity with the following four reductants: iron(II)sulfamate [21], uranium(IV)nitrate [22], hydroxylammonium nitrate [23], and electroreduction within the extractor [24]. Generally U(IV) is added as a reducing agent during extraction according to the following equation

$$2\,Pu^{4+} + U^{4+} + 2\,H_2O \rightarrow 2\,Pu^{3+} + UO_2^{2+} + 4\,H^+$$

The external feed U(IV) process, which is usually applied in current industrial reprocessing has at least two drawbacks: (a) demand for a high U(IV) excess, and (b) occasionally failure of the process caused by the autocatalytic reoxidation of Pu(III) and U(IV) starting in the organic phase.

These facts initiated activities in different countries to develop the in situ *electroreduction*

process [25–28]. A comparison of the chemical process with the electrochemical process was made in [29] and resulted in a preference for the electroreduction process. Compared with chemical separation processes for Pu, electroreduction is simpler from both engineering and operational points of view. The process has all the advantages of the externally fed U(IV) process but avoids its drawbacks.

Because of its simplicity and compactness, also *electrooxidation* has significant advantages when compared to the chemical oxidation process.

Titanium, platinum, and hafnium show sufficiently low corrosion rates to guarantee a long life-time of the electroredox equipment. Since the first electroreduction experiments performed at Forschungszentrum Karlsruhe, efforts to design simple, compact and reliable electroredox equipment for industrial applications led to the following three design criteria [24]: (a) no diaphragm, (b) casing of apparatus used as cathode, and (c) operation at constant current or voltage.

Basic chemical investigations and corrosion tests of different materials showed that these criteria can be fulfilled for both the electroreduction extractors and the electrooxidation cell [24, 30]. Diaphragms are not necessary because of the irreversible character of the U(VI) electroreduction in the used electrolyte [31] and of the hydrazine electrooxidation. Titanium was found to be well suited as the container and cathode material, having corrosion rates of less than 50 μm per year under process conditions. Experiments with constant current or voltage operation showed that side-reactions such as hydrogen formation and nitrate reduction can be suppressed to a tolerable level, so that reference electrodes are not required for constant voltage operation.

5.2. Electroreduction Processes

In the electroreduction processes plutonium is reduced by electrolysis at the cathode

$$Pu^{4+} + e^- \rightarrow Pu^{3+} \; 0.92\,V$$

and by U(IV) generated in-situ.

The local uranium : plutonium ratio in the extractor determines which reaction is dominant. The Pu(III) is reoxidized in both phases by nitrite in an autocatalytic reaction [34]:

$$Pu^{3+} + HNO_2 + H^+ \rightarrow Pu^{4+} + NO + H_2O$$

For this reason, the aqueous phase is stabilized with hydrazine, which reacts with nitrous acid

$$N_2H_5^+ + HNO_2 \rightarrow HN_3 + 2\,H_2O + H^+$$

$$N_2H_5^+ + 2\,HNO_2 \rightarrow N_2 + N_2O + 3\,H_2O + H^+$$

Since hydrazine is not extractable, a part of the Pu(III) is oxidized by organic nitrite, which results in an excessive U(IV) consumption, [43].

$$N_2 + 5\,H^+ + 4\,e^- - N_2H_5^+ - 0.23\,V$$

Hydrazine itself slowly reduces Pu(IV):

$$4\,Pu^{4+} + N_2H_5^+ \rightarrow 4\,Pu^{3+} + N_2 + 5\,H^+$$

$$2\,Pu^{4+} + 2\,N_2H_5^+ \rightarrow 2\,Pu^{3+} + 2\,NH_4^+ + N_2 + 2\,H^+$$

The last reaction is catalyzed by platinum, which is available because of corrosion of the anode [41].

Mixer-Settler. Figure 16 shows schematically the construction of the electroredox mixer-

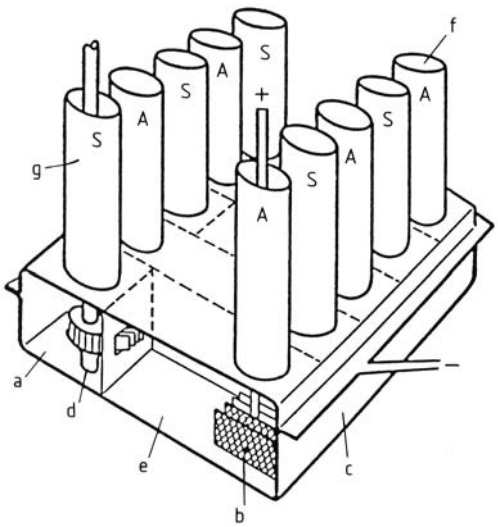

Figure 16. Electroreduction mixer – settler (1 B unit) at Karlsruhe Reprocessing Plant
a) Mixing chamber; b) Anode; c) Cathode; d) Stirrer; e) Settler; f) Anode stack (A); g) Stirrer stack (S)

Table 6. Results of test runs with electroreduction mixer-settlers

	Purpose of test	Flow ratio org./aq.	Pu product concentration, g/L	Separation		Voltage, V
				Pu-DF[a]	U-DF[a]	
MILLI-EMMA	U/Pu split FBR model fuel[c]	5 – 6.7	≤ 22	≤ 4500[b]	≤ 3000[b]	2.8 – 8.0
	U/Pu split LWR model fuel	7.1 – 9.3	≤ 4.8	≤ 2000[b]	≤ 3800[b]	2.8 – 8.0
	Pu purification cycle	2.0 – 3.5	≤ 46	≤ 20 000[d]		≤ 6.0
WAK-2B-EMMA	Pu purification cycle	2.0 – 3.0	≤ 36	≤ 100 000[e]		2.0 – 8.0

[a] DF = decontamination factor.
[b] 9 practical stages for Pu strip, 7 for U scrub.
[c] 20 vol % TBP, 30 vol % for all other experiments.
[d] 16 practical stages used for Pu strip, without U scrub.
[e] 12 practical stages used for Pu strip, without U scrub.

settler developed in Karlsruhe. The mixer-settler is made of titanium and the containment acts as cathode. The anodes are installed in the settler chambers where the electroreduction takes place. The most stable anode material is platinum with corrosion rates of a few micrometers per year. For industrial electroredox equipment, platinized Ta, Ti or other materials are used.

Table 6 summarizes the results of countercurrent experiments with the electroreduction mixer-settlers, called EMMA [24, 33, 34]. The 16-stages MILLI-EMMA was used for uranium-plutonium separation, as well as for plutonium purification, but without a uranium scrub in the latter case. Because of the miniature size of the apparatus, the extraction stage efficiency was low, especially in experiments with a high organic to aqueous flow ratio. The major parameter variations were: (a) TBP concentration, (b) plutonium content, (c) current density, (d) HNO_3 concentration in the aqueous strip solution, (e) dibutylphosphoric acid, $(C_4H_9O)_2POOH$ · (HDBP) concentration in the organic solvent, (f) flow ratios, and (g) total volume flow rate (residence time).

The most significant effect on the U/Pu separation was due to variations of the total volume flow rate. A decrease in the total volume flow rate causes complex interactions in the countercurrent extractor due to the increase in residence times for both phases. In the case of the miniature mixer-settler, the increase in extraction stage efficiency seems to be the dominant factor for separation improvement. In the Pu purification experiments an upper limit for the organic to aqueous flow ratio of 3 : 1 was found at Pu product concentrations of about 40 g/L.

The first industrial application was performed in the Pu purification cycle of the Wiederaufarbeitungsanlage Karlsruhe (WAK). The plant was equipped with an electroreduction mixer-settler (WAK-2B-EMMA, 12 stages) and an electrooxidation cell (WAK-2B-ROXI) in 1980 [34, 35]. In addition, in 1984, the first highly active cycle of WAK was equipped with an electroreduction mixer-settler.

In the WAK-2B-EMMA the flow ratio could not be raised above 3 : 1, corresponding to a Pu product concentration of about 36 g/L, although this apparatus has a significantly higher stage efficiency. One reason for the limitation of the Pu decontamination factor (DF) to a maximum of 10^5 are the very long residence times (volume flow limitations for technical reasons) [34, 35].

Pulsed Column. The extractor type preferred today for industrial reprocessing plants are pulsed sieve plate columns (Fig. 17). The main reason for this is the less complicated design of a critically safe pulsed column in comparison to a mixer-settler bank, at least for the U/Pu separation step. The pulsed column is constructed in a similar way to the mixer-settler. The column and the sieve plates, made of titanium, function as the cathode, while the platinized central rod is the anode. In the top decanter of the column, separator shields are installed to promote the separation of electrolytic gas from the organic liquid. The ratio of cathode to anode areas is made as large as possible to reduce anodic reoxidation of Pu(III). To eliminate any risk of a hydrogen explosion, the gas volumes of the mixer-settler and of the top decanter of the pulsed column are sparged with air to dilute the

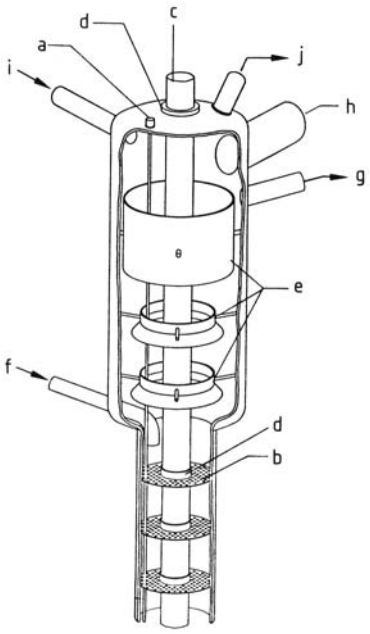

Figure 17. Pulsed electroreduction column
a) Cathode (outer casing); b) Cathode (perforated plates); c) Anode; d) Insulators; e) Gas – liquid separator plates; f) Aqueous-phase inlet; g) Organic-phase outlet; h) Overflow; i) Gas inlet; j) Off-gas outlet

hydrogen below the explosive limit. The hydrogen current yield can be kept below 10 % under typical conditions.

The first experiments with the electroreduction column ELKE done in the plutonium test facility PUTE under the conditions of a Pu purification cycle yielded decontamination factors of up to 10^6 depending on the residual uranium content, flow ratio, nitric acid concentration, etc. [36]. The effective column length was about 8 m. The following experiments were carried out to study the electroreduction feasibility in the first extraction cycle, i.e., for U/Pu separation. Based on the results achieved in the purification cycle a comparable outcome was expected for separation. However, the experiments showed a surprisingly poor separation efficiency: decontamination factors of only 200 to 2000 were achieved [37]. This was due to the fact that in the middle region of the column unusually large organic phase drops appeared with diameters of up to 20 mm and with inclusions of aqueous phase. This latter effect explained the observed insufficient U/Pu separation by heterogeneous contamination, in this case aqueous drops.

The first way to reduce the amount of entrained aqueous phase transported with the organic phase drops is an increase in pulse energy [38]. The plutonium decontamination factor increases steeply when increasing the pulse energy $A \times f$ (amplitude × frequency) from 90 to 180 cm/min. Applying a pulse energy of $A \times f = 180$ cm/min small organic drops form a homogeneous dispersion without any inclusions of aqueous phase and a maximum Pu-DF of about 12 000 is achieved with a column length of only 5 m for the reductive Pu strip (BX part, see Fig. 15). To meet the final product specification for U, a Pu-DF of about 500 000 is necessary, however. To further increase separation, two consecutive columns were used in order to extend the reductive strip height and to minimize the entrainment effect by the introduction of an intermediate decantation. The results are summarized in Table 7 [38]. Row 2 shows that the desired Pu-DF can be reached with a flow ratio of 7.25 (which is usual in this process step for LWR fuel) by the use of two combined columns with 12.6 m total length.

Furthermore, it was also shown in the experiments, that in the case of a maloperation (interrupted hydrazine feed), no inadmissibly high Pu accumulation appears. The measured maximum plutonium concentration (first column) was always less than 20 g/L within 30 h after interruption in hydrazine supply.

In the electroreduction process only small amounts of the byproducts hydrazoic acid and ammonium are formed, thus reducing the hydrazine consumption. As was demonstrated in the PUTE facility [39, 40], electroreduction has the potential to be operated without the addition of

Table 7. Results of U/Pu separation with two electroreduction columns in series*

Volume flow ratio org./aq. in BX part	Pulsation I. column, cm/min	$A \times f$ 2. Column, cm/min	[Pu] in raffinate, mg/L	Pu-DF	U-DF
6.00	135	180	$\ll 0.01$	$\gg 73\,000$	143
7.25	135	180	0.0015	507 000	345
9.33	135	180	0.005	116 000	311

* Org. feed: 88 to 90 g U + Pu per liter, [U]/[Pu] = 100, $[HNO_3] = 0.2$ M, strip solution: $[HNO_3] = 0.1$ M, $[N_2H_5^+] = 0.05$ to 0.15 M, extraction height: BX part: 6.6 m + 6 m, BS part: 1 m, volume flow ratio in BS part: 1, cathodic current density: 0.5 to 0.8 mA/cm^2.

hydrazine, if the nitric acid concentration is kept below 0.7 M within the whole extractor.

5.3. Electrooxidation

Between each cycle of the Purex process, plutonium has to be reoxidized to the tetravalent state and hydrazine must be destroyed. For this purpose an electrooxidation cell, called ROXI, was developed (Fig. 18). The anodic destruction of hydrazine is aided by the reactions of hydrazine with Pu(IV) formed by anodic oxidation and with HNO_2, which is cathodically produced in small amounts. The electrooxidation cell is a typical electrochemical flow reactor designed to minimize axial mixing. The electrolytic gas leaves the cell diluted with sparging air. The containment (cathode) is again made of titanium. The anode stacks are made of platinized metal sheets. The major advantage of electrooxidation compared to chemical oxidation with nitrogen oxides is the compactness of the apparatus. The chemical oxidation process requires one absorption column for the complete oxidation of hydrazine and Pu(III) and one additional column to desorb the excess of nitrogen oxides [32].

The yield of the direct anodic oxidation of Pu (III) depends on the nitric acid concentration. Under typical conditions, the major part of the Pu (III) is oxidized autocatalytically by HNO_2. The accompanying U(IV) is consumed by reduction of Pu(IV).

The formation of Pu(VI) is suppressed at a HNO_3 concentration higher than 2 M. The formation of ammonium by cathodic reduction of HNO_3 depends on the electrolyte composition and was measured to be 0.03 to 0.46 mmol A^{-1} h^{-1} for an electrolyte without hydrazine [41].

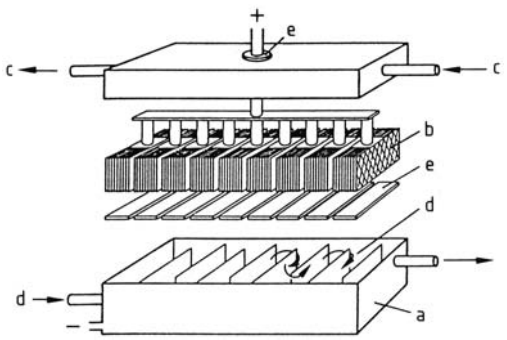

Figure 18. Electro-oxidation cell for plutonium(III) and hydrazine
a) Cathode and housing; b) Anode; c) Gas flow; d) Electrolyte flow; e) Insulation

Table 8. Average results of electrooxidation cells in PUTE

Apparatus	$N_2H_5^+$ current consumption, Ah/mol	Pu(VI) formation, % of Pu	NH_4^+ formation, mmol A^{-1} h^{-1}
Titanium-ROXI	≤ 100	≤ 2	≈ 1
Hafnium-ROXI	≤ 170	≤ 2	0.1 – 2
Hafnium-ROXI	≈ 150	~ 1	≈ 0.6

The average values achieved with the two electrooxidation cells installed in the PUTE facility are given in Table 8. For typical feed compositions, current consumption of about 100 A h per mole $N_2H_5^+$ were measured in the Ti-ROXI. For the Hf-ROXI, a higher current demand was measured, which is probably caused by a smaller fraction of cathodic reaction supporting the hydrazine destruction. The ammonium formation is low but in some cases still higher than expected. This can be explained by the formation of ammonium in parallel to the electroreduction of HNO_3.

5.4. Corrosion

The corrosion of titanium under cathodic conditions depends on the electrolyte composition and on the current density. For the relevant and maximum HNO_3 concentration of 2.5 M, gravimetric experiments show a drastic decrease in corrosion in the presence of reducible cations; no definite effects of current density are detected in this case. Traces analysis in the product solutions confirm this effect for various pieces of equipment. Only a small increase in corrosion is observed at higher ROXI current densities. Thickness measurements of the PUTE-ROXI channel sheets show, after an operation period of 1950 h, comparably small corrosion rates of 23 μm/a even at current densities up to 135 mA/cm^2. The corrosion rate of hafnium, estimated from traces analysis, amounts to 7.7 μm/a at current densities of 50 mA/cm^2.

The anodic corrosion of platinum increases with decreasing nitric acid concentration and with increasing current density and temperature [42]. The corrosion rates obtained by

gravimetric, trace and neutron activation analysis for typical electrolyte compositions and current densities amount to a few micrometers per year.

6. Electrochemical Water and Effluent Treatment

6.1. Cathodic Treatment

Wastewater from different industrial sectors, such as electroplating, photographic development, printed circuit board production, or battery technology, requires special treatment to remove toxic metal ions or to recycle valuable material. Due to increasingly stricter regulations for the discharge of effluents, the permissible concentration of metal ions in effluents has been strongly decreased in recent years [44–46]. Table 9 shows the development of the limiting values for different metal ions in Germany from 1983 until 1991 and for comparison the latest values in Switzerland. The concentrations which can be obtained by the conventional technique of hydroxide precipitation are also listed in Table 9. Obviously, the limits for effluent discharge can only be met for a few metals such as Cu or Zn by the conventional technique. Here, the precipitated metal ions are replaced by alkali or alkaline-earth metal ions and in many cases the salt content prevents the recycling and reuse of the water. Furthermore, the cost of disposing sludge containing toxic metals has also been drastically increased during recent years [47]. Costly measures are also necessary to avoid the contamination of ground water with metal ions leached out by the rain.

As an alternative to hydroxide precipitation, ion exchangers are gaining in importance; however, ion exchangers are too costly for many types of effluents, and regenerable exchange resins are not available for all metals. As a result, there is incentive to develop electrochemical processes for pollution control [48–56].

6.1.1. Optimization of Cell Design

Since most of the metal ions can be removed by cathodic deposition, electrochemical processes have been developed, some of which are already commercialized and now being used in the industry [48, 51, 53, 54]. The removal of metal ions Me^{z+} from wastewater is based on cathodic metal deposition:

$$Me^{z+}_{sol} + z^{\leftrightarrow}e^- \leftrightarrow Me$$

From a thermodynamic point of view, the Nernst equation predicts that it should be possible to decrease the Me^{z+} concentration in solution to an arbitrarily low value, if the potential E of the Me/Me^{z+} electrode is maintained sufficiently negative with respect to the standard potential $E^o_{Me/Me^{z+}}$.

$$c_{Me^{z+}} = c^+ \exp\left[\frac{zF}{RT}(E - E^o_{Me/Me^{z+}})\right] \quad (4)$$

However, at extremely low concentrations, the rate of the mass transport controlled process strongly decreases. In practice, electrolysis of metals at concentrations below 0.05 ppm (mL/m^3) is no longer economical due to increasing electrolysis time and unacceptably low space – time yield. Since the current densities at low metal ion concentrations are small, the specific energy demand for an electrochemical wastewater purification process is generally quite low,

Table 9. Effluent limits and metal concentrations obtained by hydroxide precipitation at pH 8

Metal	Effluent limits, ppm				Metal concentration after precipitation, ppm
	Germany (as of January 1983)	Germany (as of January 1991)	United States	Switzerland (1991)	
Pb	2	0.5	0.5	0.5	21
Cd	0.5	0.2	0.3	0.1	1500
Cu	2	0.5	0.5	0.5	1
Ni	3	0.5	0.5	2	340
Hg	0.05	0.05		0.01	
Ag	2	0.1		0.1	
Zn	5	2	0.5	2	2.6
Sn	5	2		2	

typically in the order of 0.025 Euro/m^3 [44]. More relevant are the specific investment costs, which are inversely proportional to the space –- time yield *STY* of the reactor. For the cathodic metal deposition in an electrochemical reactor of volume V, the space –- time yield is defined as the amount of metal dm deposited in a time interval dt:

$$STY = \frac{1}{V}\frac{\mathrm{d}m}{\mathrm{d}t} \tag{5}$$

According to Faraday's law, dm is proportional to the electrolysis charge $A\,\phi^{e}\,j\,\mathrm{d}t$:

$$\mathrm{d}m = A\phi i \mathrm{d}t\,\frac{M}{zF}e \tag{6}$$

The optimal process condition are met when the rate of the heterogeneous reaction attains its maximum at the limiting diffusion current density j_l. For a given metal ion concentration $c_{Me}{}^{z+}$ a high mass transfer coefficient k_m and a large specific electrode area are essential to obtain high space – time yields.

The reactor performance is not independent of the wastewater properties. Therefore, a normalized space velocity ϱ_s^n was introduced for the characterization of the reactor performance for a given degree of conversion [57, 68]:

$$\varrho_s^n = \frac{I\phi e}{(c_i - c_e)V\,zF}\log\frac{c_i}{c_e} \tag{7}$$

This figure gives the volume of wastewater in cubic centimeters treated by reducing the inlet concentration c_i by a factor of 10 ($c_e = 0.1\ c_i$) within 1 s in a reactor volume of 1 cm^3.

6.1.2. Electrochemical Reactors and their Applications

Different types of cell constructions have been designed during recent years. Efficient cell design has been directed towards optimizing the space – time yield, using a high specific electrode area and/or a large mass transport coefficient. With respect to these criteria, the electrochemical cells may be classified into the following three groups [44]:

Improved mass transport and thus increased current density by setting the electrodes in motion or by applying turbulence promoters, but with a relatively small electrode area in a given cell volume. Examples are the pump cell [80, 81] the Chemelec cell [58], the ECO cell [59, 60], the beat rod cell [61, 62] and cells with vibrating electrodes or electrolytes [63].

Attempts to accommodate *large electrode area* in a small cell volume resulted in developments such as the multiple cathode cell [64], the Swiss roll [65], or the extended surface electrolysis (ESE) cells [66].

Improved mass transfer coefficients and enlarged specific electrode area are provided by the use of three-dimensional electrodes. Examples are the porous flow-through cell [67], the RETEC cell [68], the packed-bed cell [69–71] the fluidized bed cell [72–76], and the rolling tube cell [77, 78]. Due to the specific fluid dynamic conditions inside these three-dimensional bed electrodes, they provide not only large specific electrode areas but also high mass transport coefficients.

Chemelec Cell. The Chemelec cell (manufactured by Bewt Water Engineers Ltd., Alcaster, UK), depicted schematically in Figure 19 uses a fluidized bed of glass spheres as turbulence promoters to improve the mass transfer to the electrodes consisting of a series of closely spaced gauze or expanded metal sheet electrodes. [58, 79]. Since the electrolyte flow velocity must exceed the minimum fluidization velocity, the residence time and the degree of conversion per pass are limited. Therefore, this cell is suitable for pretreatment or recycling operation and is commonly used in the electroplating industry for maintaining a moderate metal ion concentration

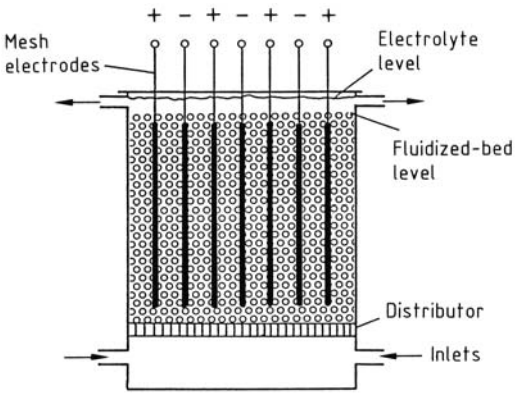

Figure 19. The Chemelec cell, with inert fluidized bed

of approx. 50 ppm in a recirculated wash water of a rinsing tank.

Cells with Rotating Cylinder Electrodes. High mass transport coefficients are also achieved in cells with rotating cylinder electrodes (RCE), and a small gap between the cylindrical cathode and anode. High rates of mass transport are experienced in the turbulent flow regime, so that RCE reactors allow metal deposition processes to take place at high speeds, even from dilute solutions. RCE reactors have been operated at diameters from 5 – 100 cm, with rotation speeds from 100 – 1500 rpm and currents from 1 A to 10 kA [80]. It is possible to design RCE reactors with scrapping devices to remove the deposited metal continuously in powder form from the cathode surface.

The *ECO cell* (Fig. 20) designed in the U.K., has already been produced and applied industrially. The cell usually has a segmented elctrolyte chamber (Fig. 20) to improve the residence time distribution by cascading. It has been used to recover silver and copper from wastewaters. The copper concentration in an 8-m^3/h effluent stream, passed over a 1.7-m^2 electrode, is reduced from 100 ppm to 2 ppm with a current of 1000 A at a current efficiency of 65 %. In this case, the power consumption per 1 m^3 of wastewater is 4.5 kW h, including the electrical energy necessary for electrode rotation.

Beat Rod Cell. The *beat rod cell* [77, 78], which is mainly used in small electroplating shops, is shown in Figure 21. Metal rods mounted into a rotating cylindrical carrier act as cathodes. Because of the rotation of the carrier, these rods beat against one another, causing mechanical release of metal, which can be collected as a powder at the bottom of the cell. Such a cell can reduce the silver content of a cyanide solution from 7.05 g/L to 3.5 mg/L in a batch operation mode.

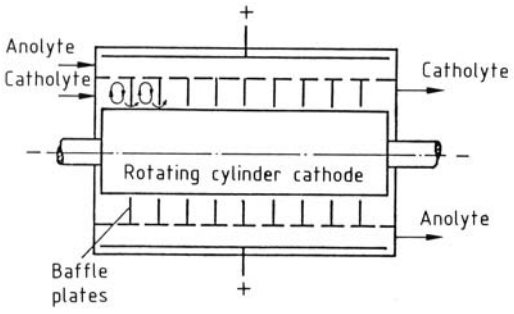

Figure 20. The ECO-cell cascade

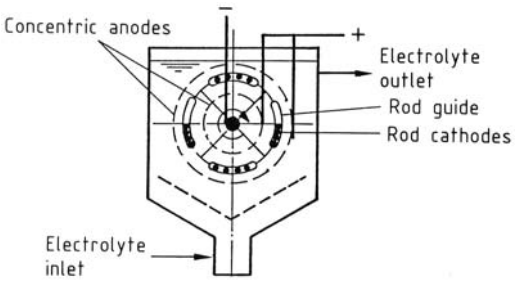

Figure 21. The beat rod cell

Swiss Roll Cell. An efficient way of fitting a large planar electrode area in a small volume is the design of the Swiss roll cell. When the cell is filled with deposited metal, it is regenerated by treatment with acid, similar to common ion exchanger resins. Large space – time yields are realized and mass transport conditions are favorable since the separator functions as a turbulence promoter. The capacity of the cell can be further increased by using perforated electrodes, thus achieving a truly three-dimensional electrode structure. Mesh electrodes wrapped around a perforated winding core, lead to another version of the Swiss roll cell with radial flow.

ESE Cells. Another design which uses mesh electrodes instead of foils is known as ESE cells. These cells have been successfully applied on an industrial scale for the purification of copper containing effluents. A quite efficient commercial system for wastewater treatment is the *RETEC cell* (Eltech System Corp., Cardon, Ohio). The design is similar to a simple tank house cell, but contains 6 – 50 three-dimensional cathodes constructed as flow-through metal sponge electrodes [68]. These cathodes have an active surface area of approximately 15 times their geometrical area. Between each pair of cathodes is placed an inert, dimensionally stable anode (DAS) which is an oxide-coated titanium mesh. The cell is used in closed water recycling systems in the electroplating industry with applications similar to those of the Chemelec cell.

Packed-bed Cells with three-dimensional electrodes are obtained when using electrodes consisting of electron conducting particulate material through which the electrolyte can flow. Numerous versions of these porous cells have been described in the literature [53, 54, 67, 81–83] (see → Electrochemistry, 3. Organic Electrochemistry Section 4.3.2. In a three-dimensional electrode the penetration depth of the current is restricted in the direction parallel to current flow. According to Equation (4), see → Electrochemistry, 3. Organic Electrochemistry Section 4.3.2, the penetration depth of the limiting current density increases as the concentration, which is proportional to j_l, decreases. The application of this principle led to the *enViro cell.* shown in Figure 22, which can operate satisfactorily at low metal ion concentrations. For example, in a single-pass operation, the concentration can be reduced from 10 – 50 mL/m^3 to less than 1 mL/m^3. This cell has a high space – time yield at a residence time of a few minutes only. The metal ion concentration can be reduced by up to a factor of 1/1000 in a single pass. The enViro cell has found wide spread industrial application (see Table 10).

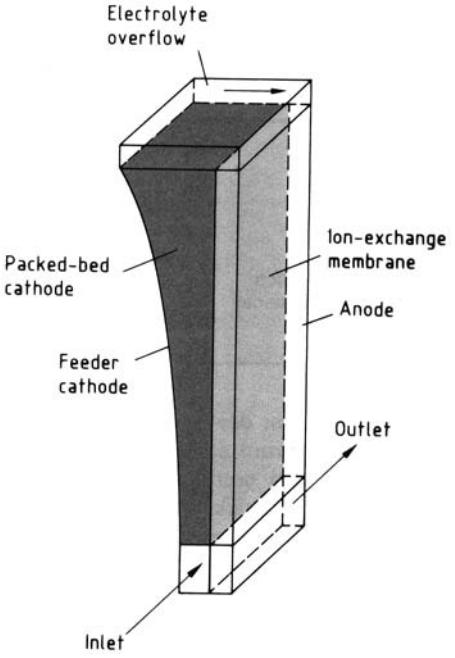

Figure 22. The enViro cell

Fluidized-Bed Electrolysis. The principle of fluidized bed electrolysis originates from FLEISCHMANN and GOODRIDGE [73]. The electrolyte flows from bottom to top through a loose bed of particles (Fig. 23). The advantage is that the particles are held in suspension, thus avoiding bed blockage as found in fixed-bed cathodes and allowing continuous metal recovery. The fluidized particles are cathodically charged via a feeder electrode. The growing particles are gathering at the lower part of the cell where they can be collected and replaced by fresh particles from the top. Because the height of the cell is restricted to about 2 m for hydraulic reasons and the fluidization velocity has to be maintained at a relatively high level, short residence times and thus only limited degree of conversion per pass can be achieved. Continuous operation with solution recirculation and cascade arrangements of cells are therefore used in practical applications.

Table 10. Applications of the enViro cell [45]

Application	Metal	Throughput, m^3/h	Concentration, ppm		Energy consumption, kW h/m^3	Anode area, m^2
			Inlet	Outlet		
Production of measuring instruments	Hg	0.3	300	0.05	1.2	1
Film processing	Ag	0.2	15	1.0	0.15	1
Salt production	Pb	0.5	2	0.1	0.07	1
Electroplating	Cd	0.2	20	1.0	0.18	1
Battery production	Hg/Cd	0.08	500	0.01	1.7	3
Cellulose acetate production	Cu	20	20	1.9	0.08	40
Pickling (recycling of solution)	Cu	3	150	50	0.19	5
Dye production	Cu	6	400	2.0	4.0	90
Dye production	Hg	2	4	0.05	2.5	15

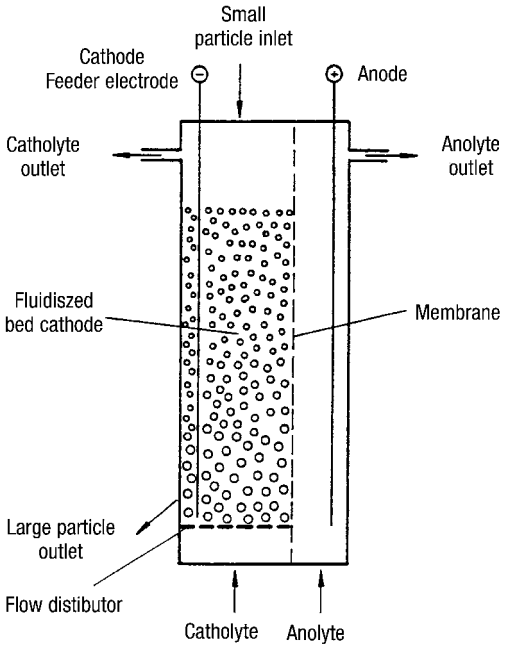

Figure 23. Fluidized-bed electrolysis according to FLEISCHMANN and GOODRIDGE

Fluidized-bed electrolysis has been examined for different applications in many laboratories, [72, 81, 82, 97, 98, 119] and has also been applied on an industrial scale for metal recovery [75, 76]. A typical example is the removal of copper from the process liquor in cellulose acetate production for membrane fabrication of artificial kidneys [44].

Moving and Circulating Bed Electrodes [83]. Figure 24 shows an example of the *rolling tube cell* [77, 78]. In principle this cell resembles the one used in the well-known plating process for piece-goods, using slowly rotating barrels. The rotating drum is only partially filled with graphite particles to achieve thorough agitation. The cathode has the shape of a perforated annular-type drum and is surrounded inside and outside by anodes to render the current distribution as homogeneous as possible. This cell is especially useful for silver and gold recovery. Further developments of moving bed cells and their application can be found in [84]. Utilization of the spouted bed, vortex bed, and moving bed electrodes for copper recovery from dilute solutions has been described in [83].

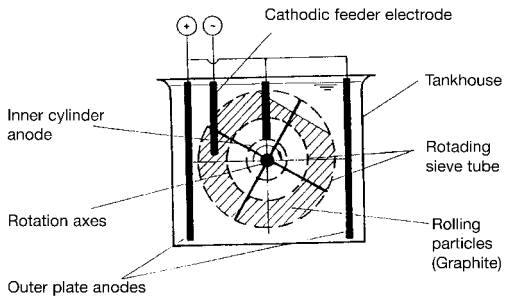

Figure 24. Rolling tube cell

Cementation Processes. [85–88]. An alternative to electrically driven cells using high surface area electrodes such as packed or fluidized-bed electrodes is a cementation system where electrochemical activity takes place spontaneously and a more noble metal may be deposited onto a less noble substrate which itself progressively dissolves [85]. Thus, no electrical energy is consumed in the precipitation reaction although power is required for electrolyte circulation. Well known examples of commercial cementation processes are the final purification step in leach liquor treatment prior to electrolysis in zinc electrowinning, where zinc dust is used as precipitant, and the recovery of silver from spent photographic solutions using steel substrates.

6.1.3. Operation Data of Electrochemical Cells

A summary of operation data of the different reactors and cell design described above is given in Table 11. Since these data are obtained from cells of different size and different process conditions, they give a rough guide rather than a reliable basis for assessing the individual reactors [44].

The data presented in Table 12, i.e., the specific electric energy demand and the normalized space velocity, are closely related to the economic efficiency [44, 46]. The specific electric energy consumption E_s^e for the treatment of 1 m^3 of effluent is relevant for the calculation of the energy costs. For cells containing rotating parts, the total energy consumption E_s^t is also specified. Considering both the specific electrical energy consumption and the normalized space

Table 11. Operation data of different types of wastewater electrolysis cells [45]

Process	Scale	Removed metal	Concentration, ppm		V_r, L	V_D, L/h	j, A/cm^2	I, A	U_c, V	ϕ^e
			Inlet	Outlet						
ECO cell	Ind.	Cu	100	2	275	8000	1000	0.059	12	0.65
Beat rod cell	Ind.	Ag	6000	4	200	12.5	125		5	0.15
Swissroll cell	Lab.	Cu	380	25	0.3	0.7	0.55	0.46×10^{-3}	1.56	0.38
Porous flow-through cell	Lab.	Cu	800	0.2	2.6	0.64	0.45	3.5×10^{-3}	1.46	0.95
Packed-bed cell	Ind.	Cu	50	0.1	4.8	50	3.2	0.76×10^{-3}	1.9	0.66
Fluidized-bed cell	Ind.	Cu	77	5	192	7000	600		3.1	0.71
Rolling tube cell	Ind.	Ag	81	0.4	40	6.9	15		6.05	0.005

Table 12. Specfic and total energy consumption and normalized space velocity of different electrolysis cells for industrial applications [45]

Process	E_s^e, kWh/m^3	E_s^t, kW h/m^3	v_s^n
ECO cell	1.5	3	20
Beat rod cell	50	60	0.2
Swiss roll cell	1.23		20
Porous flow-through cell	1.03		0.9
Packed-bed cell	0.12		28
Fluidized-bed cell	0.27		30
Rolling tube cell	14.2		0.4

velocity of processes which have already found industrial application, the packed-bed and fluidized-bed electrolysis seem to perform best.

6.2. Electrodialysis

For desalination or removal of ionic pollutants from aqueous wastewaters, electrodialysis is also useful [89–95]. The scheme for recovery of nickel salts from electroplating rinsing waters is shown in Figure 25. An electrodialysis cell is constructed

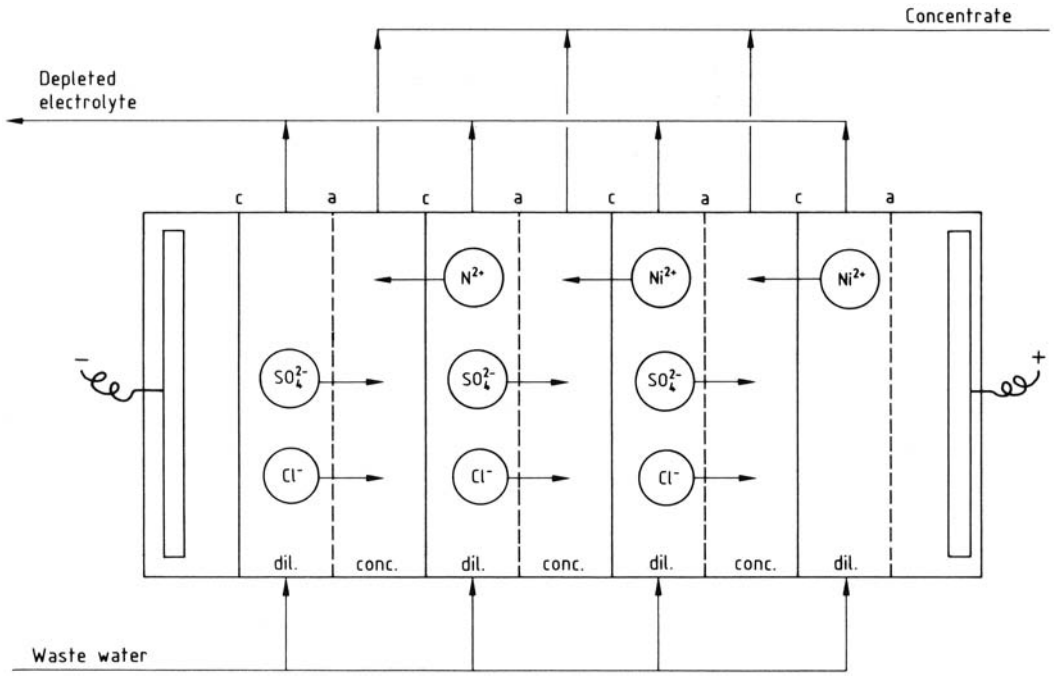

Figure 25. Nickel recovery from electroplating rinsing water by electrodialysis [93, 95]: a) Anion exchanger; c) Ccation exchanger

like a bipolar filter-press electrolyzer, but only the two end chambers of the stack are fitted with electrodes. The compartments are separated from each other alternately by cation (c) and anion (a) exchange membranes. The separation is based on the migration of ions in the electric field established by the cell voltage between the end electrodes. The material flux of a species i is $t_i\, j/z_i F$. The alternating cation and anion exchange membranes cause the contaminated electrolyte to be depleted, while the concentration, in this case of nickel and counterions, is enhanced in the concentrate. This separation is due to the fact that the transport numbers are close to unity for anions in the anion exchange membrane and for cations in the cation exchange membrane:

free electrolyte $t_i^+ \approx t_i^-$
cation membrane $t_i^+ \gg t_i^-$
anion membrane $t_i^+ \ll t_i^-$

Industrial applications have been reported, especially for nickel recovery [59, 60].

Electrodialysis does not result in the recovery of solid metals, but concentrates salt solutions. Although the concentration requirements for effluent treatment cannot be met, the concentration can be maintained on a level suitable for recirculation. Electrodialysis is generally not applicable to mixed electrolytes since suitable ion selective membranes are not available.

6.3. Anodic Treatment

By an electrochemical treatment of wastes either a partial (reduction of toxicity) or a complete decomposition of the pollutants can be achieved. In case of organic materials complete decomposition means the oxidation to carbon dioxide and as consequence a relatively high energy consumption for large organic molecules. The attempts for an electrochemical oxidizing treatment of wastewater or wastes can be classified into two categories:

Direct oxidation at the anode
Indirect oxidation using appropriate anodically formed oxidants (Cl_2, hypochlorite, peroxide, ozone, Fenton's reagent, peroxodisulfate)

A special case of indirect oxidation – frequently called *mediated electrochemical oxidation* (MEO) – is the use of metal ions with high oxidation potential (e.g., Ag(II), Co(III)) which can be electrochemically generated in a closed cycle largely avoiding emissions.

6.3.1. Direct Oxidation at the Anode

A suitable anode for direct oxidation has to meet mainly two requirements: high oxygen overpotential and corrosion stability.

A model described in [96] for the course of the anodic oxidation of an organic molecule assumes three major steps: (S indicates surface)

Discharge of water forming an adsorbed hydroxyl species:

$$S[\,]+H_2O = S[OH]+H^+ + e^-$$

The adsorbed OH is the "activated state" of water in oxygen-transfer reactions to the organic molecule R:

$$S[OH]+R = S[\,]+RO+H^+ + e^-$$

Coevolution of O_2 by oxidation of water diminishing the current efficiency:

$$S[OH]+H_2O = S[\,]+O_2+3\,H^+ + 3\,e^-$$

Phenol and its derivatives are the most frequently investigated molecules of electrochemical oxidation studies. Different anode materials such as platinum as reference electrode [97], nickel, glassy graphite, and titanium-supported oxide electrodes (IrO_2, RuO_2, PbO_2, and SnO_2 [98, 99]) and Bi as well as Fe-doped PbO_2 [96] were tested. A high oxidation rate was achieved with lead dioxide anodes using a packed-bed cell [100, 101]. The oxidation of phenol was complete at optimum conditions of pH and temperature in these experiments; the main product was carbon dioxide, benzoquinone and maleic acid were identified as byproducts.

The oxidation of numerous aromatic compounds has been investigated and for industrial wastewater treatment the use of a pilot plant equipped with Ti/SnO_2 anodes is reported [102].

Other applications that have been studied are direct anodic oxidation of sugars, alcohols, distillery effluents, dyes, aromatics, etc. [103].

For the direct oxidation of SO_2 in solution a kinetic study has been carried out using Pt, Pd, Ru, Ir, Rh, Re, and Au as anode materials [105].

The DSA PdO_x/Ti showed the highest electrocatalytic activity in these experiments whilst RuO_x – TiO_2/Ti and IrO_x – TiO_2/Ti were inactive. A problem for the oxidation of SO_2 is to avoid the formation of elemental sulfur at the cathode.

The direct anodic oxidation of SO_2 as a method for flue gas treatment has been studied at several electrodes (see, e.g., [106]). At graphite electrodes sulfate and dithionate are formed as products. A continuous neutralization of the generated acid is required in the process. Numerous fundamental investigations and even bench scale experiments have been performed for the anodic treatment of aqueous effluents containing further inorganic pollutants, e.g., cyanide [107], thiocyanate [104], and sodium dithionite [108].

6.3.2. Indirect Oxidation

The most used oxidant electrochemically generated belonging to this category is chlorine or hypochlorite, ozone is the other prominent oxidant which can be produced electrochemically. In addition peroxide, Fenton's reagent [109], and peroxodisulfate are used occasionally. ABB Ltd. and OxyTech Ltd. use hollow, cylindrical fluorocarbon-impregnated carbon anodes for ozone generation in a solid-polymer electrolyte cell [103].

As already mentioned the use of redox couples with high oxidation potential such as Ag(II)/Ag (I) (1.98 V vs. NHE) and Co(III)/Co(II) (1.82 V vs. NHE) can completely oxidize organic compounds to CO_2. Therefore this *mediated indirect oxidation method* was developed for the treatment of hazardous organic wastes containing only a limited amount of water. The oxidant is continuously generated electrochemically in a closed cycle. The method was originally used in the nuclear industry to dissolve refractory plutonium dioxide in nitric acid [110, 111]. This experience initiated the treatment of mixed (radioactive) wastes (e. g., tributyl phosphate, solvent of the Purex Process) at the Savannah River Laboratory, USA and at AEA Dounreay, UK. The successful experiments launched process development activities at the Lawrence Livermore Laboratory [112], at AEA Dounreay [113], and at the Forschungszentrum Karlsruhe [114], and the method was applied to a plurality of hazardous wastes. The principle of this process is

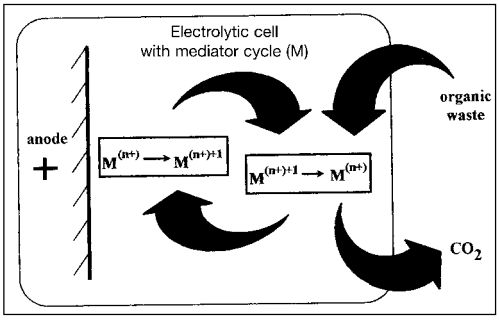

Figure 26. Principle of the MEO process

shown in Figure 26. Ag(II) is generated anodically from Ag(I) in an aqueous nitric acid solution using an electrochemical cell which is divided by a membrane. In the cathodic compartment nitric acid is reduced [115] to NO which can be regenerated to nitric acid by oxidative absorption in columns [116].

In this procedure, using two electrochemical cells, one for destruction of organics and the other for nitric acid recovery, hydrogen is the final cathodic reaction product. Investigations of Forschungszentrum Karlsruhe together with Eilenburger Elektrolyse- und Umwelttechnik have combined these two electrochemical cells into one, using silver containing nitric acid as anolyte and sulfuric acid as catholyte, thus avoiding NO formation at the cathode.

For the process development destruction experiments with different model substances and real wastes were performed both in a laboratory and in a bench-scale plant (Fig. 27). The

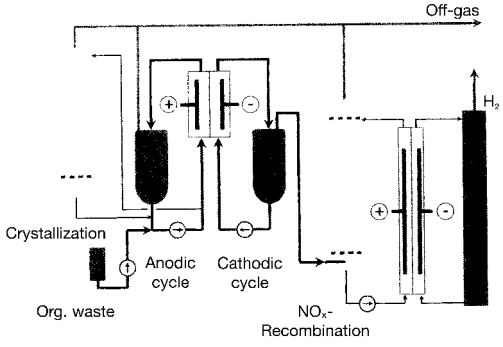

Figure 27. Bench scale MEO plant at Forschungszentrum Karlsruhe

experiments on a laboratory scale were caried out in a small filter press cell. Anode and cathode compartment were divided by a cation exchange (Nafion 450) membrane. Both electrode areas were 11 cm^2 and the volume of anode and cathode compartment was 6 cm^3 each [117]. The bench sale plant is designed similar to the laboratory plant with a scale up factor of 100. The central part of this plant consists of a monopolar electrochemical cell (ELECTROCELL AB, Sweden) or a bipolar cell from Eilenburger Elektrolyse- und Umwelttechnik GmbH (Germany). Both cells have anode and cathode areas of 0.12 m^2 each. A platinum foil anode is used, titanium or carbon serve as cathode. The maximum current density is limited by the Nafion 450 membrane to 5 kA/m^2 corresponding to a maximum current of 600 A. Liquid organic waste is fed into the anodic cycle by a pump, solid waste is fed into the anodic glass vessel from the top. Due to high flow rates of the electrolyte (up to 1500 L/h) the organic waste is finely dispersed in the electrolyte to minimize the transport inhibition at the aqueous – organic phase boundary layer [118].

In case of degradation of chlorinated organic compounds intermediate precipitates of silver chloride occur which are redissolved in presence of an excess of Ag(II) by oxidation of chloride to perchlorate, which is enriched in the anolyte and can be separated from time to time as potassium perchlorate by cooling crystallization [119].

In the laboratory plant the destruction of a large variety of different, mostly chlorinated, model substances were investigated. In all experiments the electrolyte consisted of 0.5 M $AgNO_3$/7 M HNO_3. The experiments were carried out with current densities between 1 and 5 kA/m^2 and reaction temperatures of 40 – 90 °C. All selected model substances with the exception of hexachlorobenzene could be destroyed to more than 99 %. As reaction products always CO_2 and small amounts of CO were formed.

Moreover, several organic multicomponent waste mixtures from the chemical industry were treated in the laboratory and bench scale plants. The main components were benzoyl chloride, chlorobenzoyl chlorides, chlorobenzaldehyde, benzotrichloride, and benzoic anhydride. The experiment was performed at 60 °C using a current density of 4 kA/m^2. At the start of the experiment CO_2 evolution occurred and current efficiencies up to 100 % were achieved. After 60 min CO_2 evolution decreased and O_2 formation, caused by water oxidation, increased.

Based on the described experiences and founded by the European Commission in the frame of a CRAFT project, a mobile demonstration plant was designed and built, which has been operated on an industrial site since March 1999 (Fig. 28). In case of destruction of chlorinated organic wastes, the plant offers both possibilities, separation of silver chloride from the anolyte and recovery of silver or oxidizing the

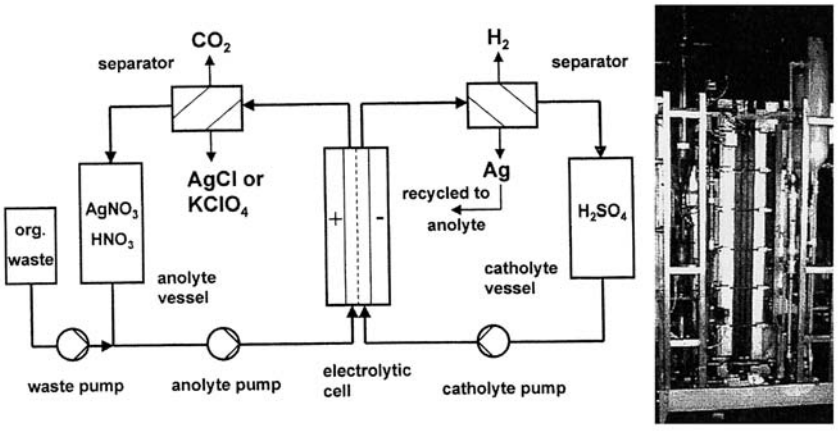

Figure 28. Mobile demonstration plant for destruction of chlorinated organic wastes

organic chlorine to perchlorate and winning of potassium perchlorate. Sulfuric acid is used as catholyte, generating hydrogen at the cathode as a valuable byproduct. The migration of silver ions from the anolyte through the membrane into the catholyte was determined to be only 0.03 g A^{-1} h^{-1}. These silver ions are reduced and deposited at the cathode, flushed out periodically, separated from the catholyte and recycled to the anolyte.

7. Electrochemical Gas Purification

7.1. General Aspects

An increasing demand for off-gas purification, particularly for smaller scale power plants, heating combustion units, or chemical plants, has encouraged the development of new concepts of electrochemical gas purification techniques. Many gaseous pollutants, such as chlorine, hydrogen sulfide, nitrous oxides, or sulfur dioxide permit electrochemical conversion in an aqueous environment, since the standard potentials of the corresponding reactions are all within the stability range of aqueous electrolytes:

$$2\,Cl^- \rightleftharpoons Cl_2 + 2\,e^- \quad E^o = 1.360\ V$$

$$H_2S \rightleftharpoons S + 2H^+ + 2\,e^- \quad E^o = 0.142\ V$$

$$NO + 2\,H_2O \rightleftharpoons NO_3^- + 4\,H^+ + 3\,e^- \quad E^o = 0.957\ V$$

$$NO_2 + H_2O \rightleftharpoons NO_3^- + 2\,H^+ + 3\,e^- \quad E^o = 0.775\ V$$

$$SO_2 + 2\,H_2O \rightleftharpoons SO_4^{2-} + 4\,H^+ + 2\,e^- \quad E^o = 0.138\ V$$

Different concepts for electrochemical gas purification can be found in the literature [45]. In any case, the initial step is absorption of the pollutant species into a liquid phase. Since the solubility of several gases in aqueous solutions is too low, the transfer from the gas phase into the aqueous phase must be supported by a reaction, which converts the primarily dissolved species permanently to a more soluble one. In the simplest case, this can occur either by direct conversion at the electrode of an electrochemical cell [119–121], or indirectly via chemical reaction with a redox mediator, which can be electrochemically regenerated in a subsequent step. Homogeneous and heterogeneous catalysts have been applied as redox mediators. The advantage of heterogeneous mediators, such as oxides, is that a separation of the reaction products from the mediator is not necessary. Both, the electrochemical conversion of the pollutant and the electrochemical regeneration of the redox mediator can be achieved either by an inner cell or an outer cell process, as illustrated in Figure 29 [123].

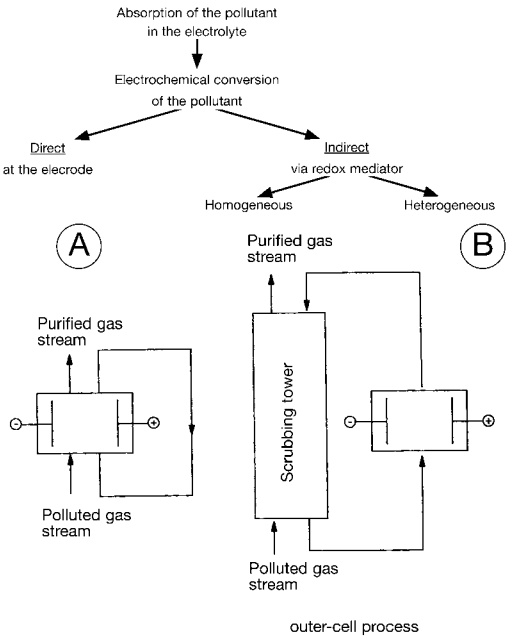

Figure 29. Electrochemical gas purification by inner cell and outer cell processes

Direct Electrochemical Conversion of gases by an inner cell process can be carried out in a specially designed electrochemical absorption column, which consists of a three-dimensional packed bed electrode of conducting particles in contact with a cylindrical feeder electrode and a counterelectrode separated by a porous diaphragm or ion exchanger membrane [119–121].

Figure 30 shows schematically the construction of such a device, which usually operates under countercurrent flow conditions of gas and liquid phases. The dissolved pollutant is directly converted at the surface of the packed bed electrode. Such a device exhibits high space – time yield and has been successfully

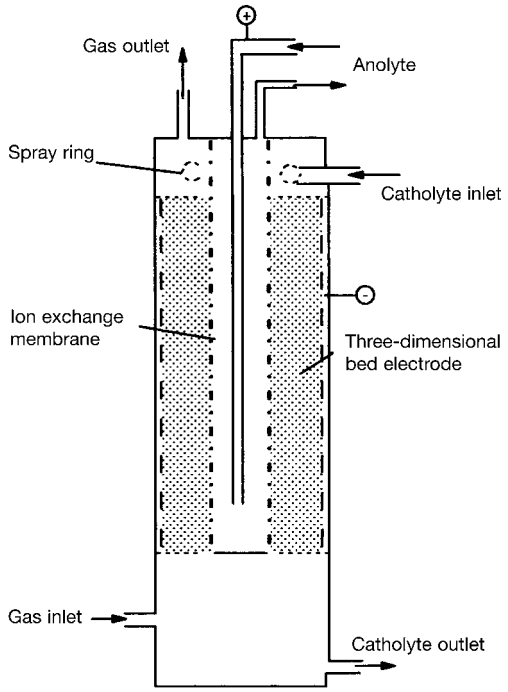

Figure 30. Scheme of an electrochemical absorption column with three-dimensional particle bed electrode

tested for electrochemical absorption of sulfur dioxide and chlorine [121, 124, 125].

Indirect Electrochemical Processes with *homogeneous redox mediator* are the so-called "Peracidox"process developed by Lurgi [126] using peroxodisulfate, and the modified "Mark 13 A" process developed at the Joint European Research Center Ispra [127], using bromine as mediator as the redox mediator for indirect SO_2 oxidation. In both cases the electrochemical regeneration of the redox mediator is performed by an outer cell process in a separate electrochemical cell.

Processes with *heterogeneous redox mediators* are the lead dioxide catalyzed oxidation of SO_2, suggested by STRAFELDA [128] and the combined electrochemical and catalytic removal of SO_2 at a Cu_2O/Cu^{2+} catalyst [129]. Porous gas diffusion electrodes have been employed for the conversion of SO_2 using pyrolyzed Co phthalocyanines as electrocatalyst [130]. Electrode technology adopted from the fuel cell technology have also been used for effluent gas treatment. A cell construction similar to that of a molten carbonate fuel cell with porous electrodes and a molten $Na_2S - Li_2S$ electrolyte at 350 °C has been examined for removal of SO_2 and H_2S [131–134]. High-temperature solid-state electrochemical cells based on Y_2O_3-stabilised ZrO_2 (YSZ) and porous palladium electrodes have been studied for the successful electrochemical removal of both NO and CH_4 at 650 – 750 °C in an oxidizing atmosphere [135]. NO is reduced to N_2 and CH_4 is oxidized to CO_x.

7.2. New Process Developments

Since flue gases not only contain SO_2 but to a certain extent also NO_x, the development of processes for the simultaneous removal of both components has been the subject of recent investigations [125, 136–139].

The Cerium(IV)-assisted Process [136, 137] is an indirect outer cell process with Ce^{4+} as homogeneous redox mediator for the simultaneous oxidation of SO_2 and NO_x to sulfuric acid and nitric acid. The acidic solution is continuously fed down to the anode compartment of an electrochemical cell where Ce^{4+} is regenerated. When the solution has reached a critical concentration of approx. 30 – 40 % HNO_3 and H_2SO_4, separation of the nitrate effluent from the sulfate solution and recycling of Ce^{3+} are performed in a separate unit, where the nitric acid is first separated by distillation and the excess of sulfuric acid is then continuously removed by liquid – liquid extraction [140, 141].

The Lead Dioxide Dithionite Process [125, 138, 139] combines direct and indirect conversion of SO_2 and NO_x, respectively, in two steps with dithionite as homogeneous redox mediator for the indirect reduction of NO_x and lead dioxide as heterogeneous catalyst and mediator for the direct oxidation of SO_2. The gas mixture first enters an absorption column, where NO is absorbed by the complexing agent Fe(II)EDTA and simultaneously reduced with dithionite. Dithionite is continuously regenerated by cathodic reduction of SO_3^{2-} in an electrochemical cell. The second component, SO_2, passes the NO

absorption column without reaction and enters an electrochemical cell, for example as shown in Fig. 30, where it is oxidized directly to sulfuric acid at the anode. A pilot plant for the treatment of 100 m^3/h (STP) of flue gas with 600 ppm NO inlet concentration had been tested on an industrial site (Brite Project 2026).

Microkinetic studies of NO_x absorption revealed that the degree of NO conversion can be significantly improved, if Fe(II)EDTA is present in the absorption solution at a low content. Another interesting aspect of electrochemical promotion of environmentally important heterogeneous gas phase reactions is the so called NEMCA effect (non-faradaic electrochemical modification of catalytic activity). NEMCA significantly increases the catalytic activity and selectivity of metal and metal oxide catalysts deposited on solid electrolytes such as YSZ or β''-Al_2O_3 by electrochemical polarization of the catalyst electrode [142–144]. Technical applications are still in the initial stage of development.

8. Electrochemical Shaping

Shaping pieces of metal by controlled anodic dissolution – controlled with respect to dissolution depth in three dimensions – is the essential aspect of electrochemical metal shaping [145–147]. This technique includes electropolishing, electrolytic or electrochemical grinding, and electrochemical machining. The last, electrochemical machining, is the fastest, most vigorous form of spatially controlled anodic metal dissolution.

Anodic corrosion, the fundamental phenomenon behind these three techniques, is characterized by the shape of the current – voltage curve in Figure 31. Anodic dissolution, which proceeds at a sizable rate in the subpassive voltage region, increases with anodic polarization. Its rate drops sharply, by several orders of magnitude, at the passivation potential, at which a dense semiconducting oxide hydrate film forms, and prevents further dissolution. At much higher potentials, however, this film breaks down, and vigorous transpassive dissolution of the metal is observed [145, 148]. If a compound of low solubility precipitates on the surface as a more or less porous deposit, instead of a passivating film, then anodic dissolution is inhibited, but the current density remains several orders of magnitudes higher than in the case of passivation. In such cases anodic dissolution usually is limited by mass transfer of the corrosion products through the pores of the deposited layer.

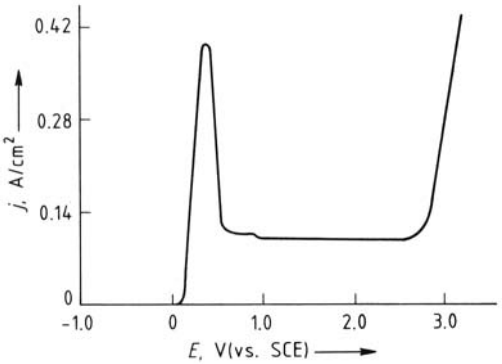

Figure 31. Voltammogram of nickel, a passivating metal, in 9 M HCl [146]

This mass tranfer-controlled dissolution through layers of precipitates is the principle governing electropolishing (Fig. 32 A), whereas transpassive high current density corrosion is used for electrochemical machining and electrochemical grinding (Fig. 32 B and C). Electrochemical grinding, which combines anodic dissolution with limited mechanical grinding is advantageous whenever a component of the alloy is not dissolved electrochemically but sticks to the surface and must be removed continuously along with the base metal. This is the case for cemented carbides as well as nitrides and borides of transition metals or refractory metals.

For processing superalloys and refractory metals, which came into use in the aerospace industry and for the construction of steam and gas turbines in the 1960s and early 1970s, the electrochemical methods – electrochemical machining, electrochemical grinding, and electrochemical polishing – are especially suitable. These methods, with the exception of electropolishing, are not likely to replace mechanical processing of conventional metals and alloys because the electrochemical techniques are expensive and too sophisticated to be used for softer alloys.

Electropolishing. Figure 31 shows the current – voltage curve for anodic dissolution of nickel in 9-N HCl solution with a limiting current

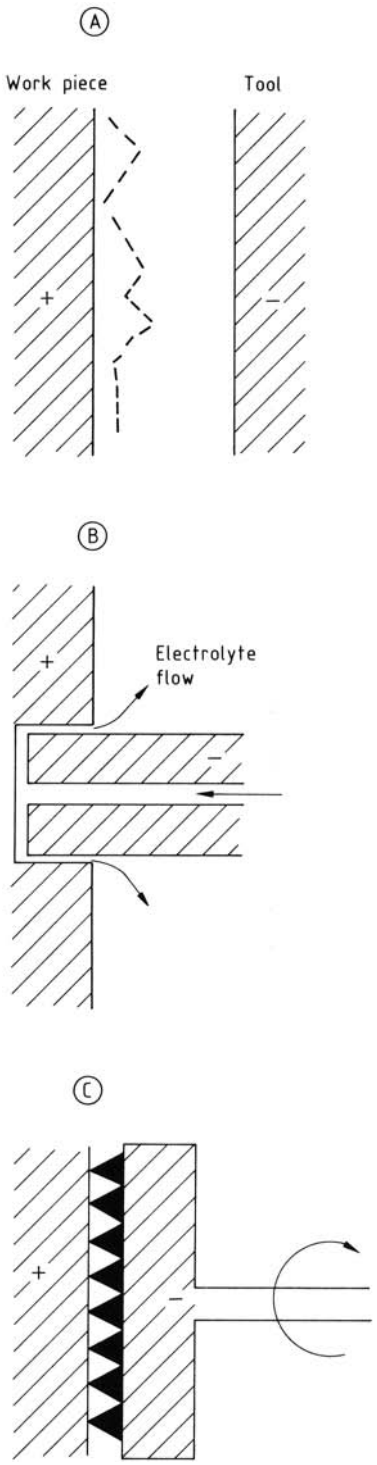

Figure 32. Schematic electrochemical shaping
A) Electrochemical polishing (– – – initial contour); B) Electrochemical machining; C) Electrochemical grinding

density of the order of 100 mA/cm^2. This mass transfer-controlled dissolution rate is caused by formation of a relatively thin layer of porous oxide hydrate. The metal cations that are formed by anodic dissolution can leave the metal surface only by diffusion through pores. Since there is good reason to believe that the pores are randomly distributed and formed and closed at random, dissolution should also be random with no preference for particular crystal faces. Consequently, etch patterns are not observed.

The polishing effect is attributed to higher local dissolution rates of the elevated parts of the initially rough surface because of the lesser thickness of the porous oxide hydrates there. Table 13 lists the conditions and electrolyte compositions for electropolishing of metals. All the electrolytes contain components or establish a pH that causes the formation of only moderatey soluble oxide hydrates or salt deposits. Such deposits form on the metal surface under steady-state conditions at current densities of ca. 300 – 3000 mA/cm^2.

Electrochemical Machining (ECM). For a practical electrochemical machining process, the metal must be removed at a cutting rate of 0.25 cm/min or more, corresponding to current densities $>$ 160 A/cm^2. At these current densities, the electrolyte gap between the cathode and the workpiece must be adjusted continually to 0.005 – 0.13 cm to conserve electric energy. In addition, the anodically generated metal ions, hydroxides, and debris, the cathodically evolved hydrogen, and the dissipated Joule heat must be removed efficiently by vigorously pumping the electrolyte through the narrow gap between the cathode and workpiece. In order to keep ohmic voltage drop across the interelectrodic gap as low as possible, the electrolytes must have high conductivity.

Commercial ECM machines apply a maximum voltage. This is distributed between the sum of the anodic and the cathodic overpotentials, which determines the current density and hence the dissolution rate, and the ohmic voltage drop across the interelectrodic gap. The ohmic voltage drop increases with gap width and current density. Therefore, for every cutting rate and voltage there is one gap width that is self-adjusting and that can be kept steady during the process, the so-called equilibrium gap.

Table 13. Electrolytes for electropolishing metals [146]

Metal	Electrolyte	Current density, mA/cm^2	Temperature, °C	Polishing time, min
Aluminum	20 wt % $HClO_4$ + 80 wt % acetic anhydride*	200 – 400	≤38	15
Copper	63 wt % H_3PO_4 + 37 wt % H_2O	20 – 50	22	5
	65 wt % H_3PO_4 + 15 wt % H_2SO_4 + 6 wt % CrO_3 + 14 wt % H_2O	200 – 250	22 – 25	2 – 5
Lead	30 vol % $HClO_4$ + 70 vol % glacial acetic acid*	1300 – 1600	22	5
Nickel	73 wt % H_2SO_4 + 27 wt % H_2O	1000 – 3000	22	2
	65 wt % H_3PO_4 + 15 wt % H_2SO_4 + 6 wt % CrO_3 + 14 wt % H_2O	200 – 250	22 – 25	2 – 5
Tin	20 vol % $HClO_4$ + 80 vol % acetic anhydride	600 – 1000	32	8 – 10
Tungsten	10 wt % $NaNO_3$ + 90 wt % H_2O	200 – 400	22	20 – 30
	Na_3PO_4 (160 g/L)	600	38 – 49	10
Zinc	25 wt % KOH + 75 wt % H_2O	1000	22	15
	17 wt % CrO_3 + 83 wt % H_2O	2000		
Brass	16 wt % CrO_3 + 84 wt % H_2O	2000		
	70 wt % H_3PO_4 + 30 wt % H_2O	500	26	5
Steel, carbon	48 wt % H_3PO_4 + 40 wt % H_2SO_4 + 12 wt % H_2O	3000	35 – 49	10
	10 wt % $HClO_4$ + 90 wt % glacial acetic acid	1500 – 2500	26	0.5 – 2
Steel, stainless	30 wt % H_3PO_4 + 60 wt % H_2SO_4 + 10 wt % H_2O	1800	49	2
	42 wt % H_3PO_4 + 45 wt % glycerol + 13 wt % H_2O	100 – 600	93 – 149	8 – 15

*Especially hazardous.

Nevertheless, short circuits, which can severely damage the tool, must be avoided, and most ECM machines are protected against such damage by special sensing devices and ultrafast electronic switches.

Figure 33 shows how electrochemical machining works in the case of electrochemical drilling or sinking. The tool is a cylindrical cathode, the wall of which is covered with an electrically insulating coating. Current densities around 300 A/cm^2 flow between the bottom of the hole and the cathode, and a vigorous stream of electrolyte flushes the dissolved metal ions and solids out of the hole.

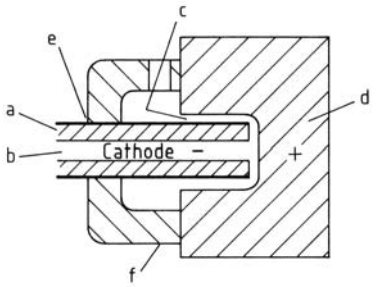

Figure 33. Schematic electrochemical sinking machine [146]
a) Cathodic tool; b) Electrolyte inlet; c) Electrolyte outlet; d) Anodic workpiece; e) Insulating coating; f) Shield

Immediately behind the cathode face there is a region where electropolishing takes place because of the reduced current densities. Consequently, electrochemical machining in most cases produces an excellent furnace finish.

Most important for successful electrochemical machining is the choice of the electrolyte. Its composition should allow metal dissolution with current densites up to several hundred amperes per square centimeter while preventing the precipitation of insoluble salts and oxides. Alkali-metal chlorates and perchlorates, which can be hazardous, have proved to be suitable ECM electrolytes. Table 14 lists the electrolyte and its concentration in typical ECM electrolytes.

Electrochemical machining became popular for processing high-strength metals and alloys and refractory metals. Some of the procedures for which ECM can be used are shown schematically in Figure 34. Die sinking is also possible. Sinking the cathode tool into the workpiece produces the cavity used for casting.

In all these operations overcuts due to the action of stray currents cannot be avoided. Computed current-density distributions have always turned out to be insufficiently accurate to prevent the overcuts. Shaping is carried out by empirically changing the tool dimensions,

Table 14. Electrolytes for electrochemical machining [146]

Metal	Electrolyte	Remarks
Aluminum and aluminum alloys	$NaNO_3$ (100 – 400 g/L)	excellent surface finish
Cobalt and cobalt alloys	$NaClO_3$ (100 – 600 g/L)	
Molybdenum	NaOH(40 – 100 g/L)	NaOH consumed and must be added continuously
Nickel and nickel alloys	$NaNO_3$ (100 – 400 g/L)	
	$NaClO_3$ (100 – 600 g/L)	good surface finish, good dimensional control, low metal removal rate
Titanium and titanium alloys	NaCl (180 g/L) + NaBr (60 g/L) + NaF (2.5 g/L)	good surface finish, good dimensional control, good machining rate
	$NaClO_3$ (100 – 600 g/L)	
Tungsten	NaOH (40 – 100 g/L)	NaOH is consumed and must be added continuously
Steel and iron alloys	$NaClO_3$ (100 – 600 g/L)	excellent dimensional control, brilliant surface finish, high
	$NaClO_3$ (100 – 400 g/L)	metal removal rate, fire hazard when dry
	$NaNO_3$ (100 – 400 g/L)	

current density, electrolyte concentration, electrolyte flow velocity, etc.

Electrochemical Grinding. Diamonds, α-alumina (corundum), or another hard material, the grinding powder, is embedded into the surface of a grinding wheel of copper or copper bronze, which serves as the cathode. The grinding powder is pressed into the metal surface and held in place by plating the studded surface with a layer of nickel. With an optimum load of 3.0 carats/cm^2, the grinding powder is exposed to a height of only 10 to 60 μm by etching the nickel away in an electropolishing bath.

The diamond (or corundum) grains do not serve themselves for grinding, but rather define and maintain the width of the electrolyte gap between the grinding wheel and the workpiece. Therefore, only light pressure is used to press the grinding wheel and the workpiece together.

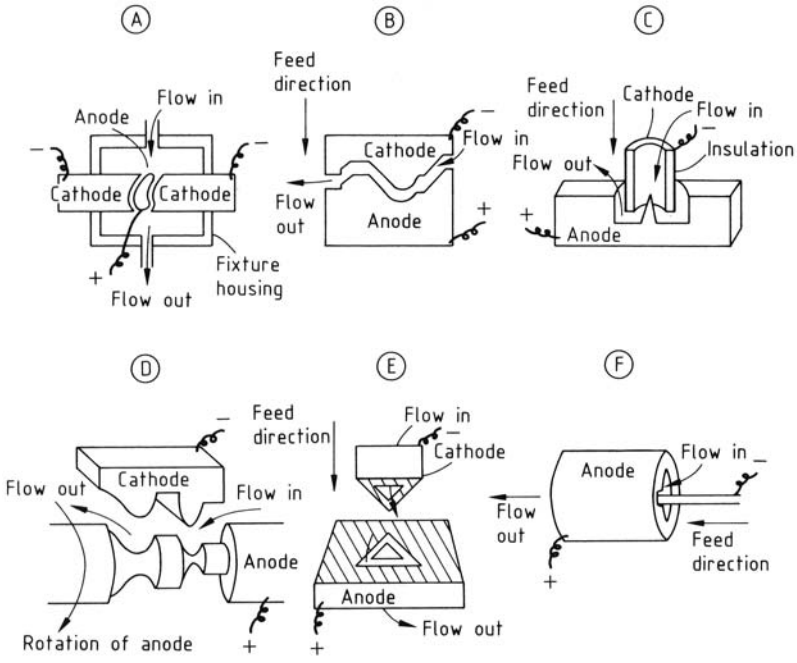

Figure 34. Sketches of various electrochemical machining operations [146]
A) External shaping; B) Cavity sinking; C) Plunge cutting; D) Turning; E) Trepanning; F) Internal grooving

Around 90 % of the metal is removed by anodic dissolution. Fully hardened steels can be processed without difficulty and without detectable wear of the tools because nearly 100 % of the metal is removed by anodic dissolution. Current densities of 12 – 40 A/cm^2 approach those used for ECM; mixtures of chlorides and nitrates serve as electrolytes. Vigorous pumping and copious electrolyte exchange is vital for electrochemical grinding.

Unlike mechanical grinding, electrochemical grinding leaves no scratches, grooves, or tool registry marks. Current densities must not be too high if increased surface roughness is to be avoided.

References

Specific References

1 H. B. Beer, *J. Electrochem. Soc.* **127** (1980) 303 C – 305 C.
2 D. L. Caldwell, *Compr. Treatise Electrochem.* **2** (1981) .
3 E. Yeager, P. Bindra, *Chem. Ing. Tech.* **52** (1980) 384 – 391.
4 H. Wendt, *Chem. Ing. Tech.* **56** (1984) 265 – 272.
5 A. Bulan, F. Gestermann, T. Turek, R. Weber, P. Weuta: *Chlorelektrolysen mit Gasdiffusionselektroden*, GVC-DECHEMA-Jahrestagungen, Karlsruhe 2004.
6 J. Jörissen: *Anwendung von Gasdiffusionselektroden bei chemischen Synthesen*, GVC-DECHEMA-Jahrestagungen, Karlsruhe 2004.
7 D. Hoormann, J. Jörissen, H. Pütter: Elektrochemische Verfahren – Neuentwicklungen und Tendenzen, *Chem. Ing. Tech.* **77** (2005) 1363 – 1376.
8 J. Müller, K. Lohrberg, H. Wüllenweber, *Chem. Ing. Tech.* **52** (1980) 435 – 436.
9 T. A. Liederbach, A. M. Greenberg, V. H. Thomas: "Commercial Application of Cathode Coatings in Electrolytic Chlorine Cells," in M. O. Coulter (ed.): *Modern Chloralkali Technology*,Ellis Horwood Ltd. 1980, pp. 145 – 149.
10 D. Dobos: *Electrochemical Data*,Elsevier, Amsterdam-Oxford-New York 1975, p. 247.
11 V. A. Ettel, B. V. Tilak: "Electrolytic Refining and Winning of Metals," *Compr. Treatise Electrochem.* **2** (1981) 327 – 380.
12 A. Schmidt: *Angewandte Elektrochemie*,Verlag Chemie, Weinheim, Germany 1976, p. 207.
13 *Elektrolyse der Nichteisenmetalle*,Verlag Chemie, Weinheim-New York 1986.
14 W. E. Haupin, W. B. Frank: "Electrometallurgy of Aluminum," *Compr. Treatise Electrochem.* **2** (1981) 301 – 325.
15 K. Grjotheim, C. Krohn, M. Malinovsky, K. Matiasovsky, J. Thonstad: *Aluminium Electrolysis*,2nd ed., Aluminium Verlag, Düsseldorf 1982, pp. 28 – 29.
16 R. Bunsen, *Poggendorf Annalen* **92** (1954) 648 –651.
17 H. Wendt, K. Reuhl, *Aluminium (Düsseldorf)* **61** (1985) 518 – 521, 592 – 597.
18 W. E. Cowley: "The Alkali Metals," in D. Lovering (ed.): *Molten Salt Technology*,Plenum Press, New York 1982, pp. 57 – 90.
19 L. Stieglitz, R. Becker, *KFK report* **3740** (1984).
20 Z. Kolarik, H.-J. Bleyl, H. Schmieder, *Proceedings of International Conference on 'Solvent Extraction'*, ISEC'86, Munich (1986).
21 C. S. Schlea, M. R. Caverny, H. E. Henry, W. J. Jenkins, USAEC-Report, DP808 (1963).
22 H. A. C. McKay, R. J. W. Streeton, A. G. Wain, UKAEA report, AERE-R 4381 (1963).
23 M. J. McKibber, J. E. Bercaw, USAEC report, DP1284 (1970).
24 H. Schmieder, F. Baumgärtner, H. Goldacker, H. Hausberger, KFK report **2082** (1974).
25 F. Baumgärtner, E. Schwind, P. Schlosser, *German Patent 1905 51* (1970).
26 A. Schneider, A. L. Ayers, *US patent 3616 276* (1971).
27 M. Krumpelt, J. Heiberger, M. J. Steindler, USAEC report ANL-7799 (1971).
28 J. P. Charvillat, J. J. Fabre, M. Le Bouhellec, M. Henry, *Proc. Extraction'84*, Dounreay, 27 – 29 Nov. (1984) , EFCE Publ., series no. **43**.
29 G. Petrich, H. Schmieder, *Proceedings of the International Conference on 'Solvent Extraction'*, ISEC'83, Denver, Co. Aug. (1983).
30 F. Baumgärtner, H. Schmieder, *Radiochim. Acta* **25** (1978) 191 – 220.
31 B. McDuffie, C. N. Reilly, *Anal. Chem.* **38** (1966) 1881.
32 H. Schmieder, H. Goldacker, M. Heilgeist, G. Petrich, *Fast Reactor Fuel Cycle*,vol. 47, British Energy Society, London 1981.
33 H. Schmieder, Ph. D. Thesis, Institut National Polytechnique de Grenoble (1984).
34 H. Schmieder, H. Goldacker, M. Heilgeist, M. Kluth, H. Hausberger, L. Finsterwalder, KFK report **2957** (1980).
35 H. Goldacker, H. Hausberger, H. Schmieder, H. Wiese, *Proc. ANS-Conf.*, Sept. (1980) , Gatlinburg, USA.
36 H. Schmieder, H. Goldacker, *Proceedings of the International Conference on 'Solvent Extraction'*, ISEC'86, Munich, Sept. (1986).
37 U. Galla, H. Schmieder, KFK report **4177** (1987).
38 U. Galla, H. Goldacker, R. Schlenker, H. Schmieder, *Separa. Sci. & Technol.* **25** (1990) 1751.
39 G. Petrich, H. Schmieder, *Proceedings of the International Conference on 'Solvent Extraction'*, ISEC'88, Moscow, July (1988).
40 M. Heilgeist, K. Flory, U. Galla, H. Schmieder, *Proceedings of the International Conference on 'Solvent Extraction'*, ISEC'86, Munich, Sept. (1986).
41 M. Heilgeist, KFK report **3517** (1983).

42 V. P. Caracciolo, A. A. Kishbaugh, USAEC report, DP-896 (1964).
43 H. Schmieder, H. Goldacker, G. Petrich, *DECHEMA Monogr.* **94** (1983) .
44 G. Kreysa, in S. Stucki (ed.): *Process Technologies for Water Treatment*,Plenum Publishing Corporation, 1988, p. 65.
45 G. Kreysa, K. Jüttner, in F. Lapique, A. Storck, A. A. Wragg (eds.): *Electrochemical Engineering and Energy*, Plenum Press, New York, 1994.
46 K. J. Müller, G. Kreysa, *Dechema Monographien* **98** (1985) 367.
47 B. von Felten, *Oberfläche Surface* (1990) no. 6, 8.
48 A. T. Kuhn, *Chem. Ind. (London)* 1971, 946 – 950.
49 D. S. Flett, D. Pearson, *Chem. Ind. (London)* 1975, 639 – 645.
50 R. Kammel, H.-W. Lieber, *Galvanotechnik* **68** (1977) 883 – 886.
51 R. Kammel, H.-W. Lieber, *Galvanotechnik* **69** (1978) 317 – 324, 624 – 630.
52 A. T. Kuhn, *Chem. Ind. (London)* 1978, 447 – 453.
53 G. Kreysa, *Chem. Ing. Tech.* **50** (1978) 332 – 337.
54 G. Kreysa, *Metalloberfläche* **34** (1980) 494 – 501.
55 C. Fabjan, *Oberfläche-Surf.* **21** (1980) 283 – 292.
56 W. Samhaber, *Chem. Ing. Tech.* **56** (1984) 246 – 247.
57 G. Kreysa, *Electrochim. Acta* **26** (1981) 1693.
58 C. L. Lopez-Cacicedo, *Inst. Chem. Eng. Symp. Ser.* **42** (1975) 29 – 31.
59 D. R. Gabe, *J. Appl. Electrochem.* **4** (1974) 91.
60 L. J. Ricci, *Chem. Eng.* (1975) 29.
61 R. Kammel, H.-W. Lieber, *Galvanotechnik* **68** (1977) 710.
62 W. Götzelmann, *Galvanotechnik* **68** (1977) 789.
63 EPA 86109265.8, 1986 (D. Bruhn, W. Dietz, K.-J. Müller, C. Reynvaan).
64 A. Storck, P. M. Robertson, N. Ibl, *Electrochim. Acta* **24** (1979) 373 – 380.
65 P. M. Robertson, B. Scholder, G. Theis, N. Ibl, *Chem. Ind. (London)* 1978, 459 – 465.
66 K. B. Keating, J. M. Williams, *Resour. Recovery Conserv.* **2** (1976) 39 – 50.
67 D. N. Bennion, J. Newman, *J. Appl. Electrochem.* **2** (1972) 113.
68 D. Pletcher, F. Walsh (eds.): *Industrial Electrochemistry*,Chapman and Hall, London – New York, 1990.
69 G. Kreysa, *Chem.-Ing.-Tech.* **55** (1983) 23.
70 G. Kreysa, C. Reynvaan, *J. Appl. Electrochem.* **12** (1982) 241.
71 DE 2 622 497, 1976 (G. Kreysa).
72 J. R. Backhurst, J. M. Coulson, F. Goodbridge, R. E. Plimley, M. Fleischmann, *J. Electrochem. Soc.* **116** (1969) 1600.
73 GB 1 194 181, 1970 (J. R. Backhurst, M. Fleischmann, F. Goodbridge, R. E. Plimley).
74 DE 2 227 084, 1972 (H. Scharf).
75 C. Raats, H. Boon, W. Eveleens, *Erzmetall* **30** (1977) 365.
76 G. v. Heiden, C. Raats, H. Boon, *Chem. Ind.* (1978) 465.
77 R. Kammel, H.-W. Lieber, *Galvanotechnik* **69** (1978) 687 – 693.
78 W. Götzelmann, *Galvanotechnik* **70** (1979) 596 – 603.
79 C. L. Lopez-Cacicedo, GB 1 423 369, 1973.
80 D. R. Gabe, F. C. Walsh, *Trans. IchemE* 68 B (1990) 107.
81 D. S. Flett, *Chem. Ind.* (1971) 300.
82 G. Kreysa, *Erzmetall* **28** (1975) 440.
83 K. Scott, *J. Appl. Electrochem.* **18** (1988) 504.
84 H. Bergmann, H. Hertwig, F. Nieber, *Chem. Eng. Proc.* **31** (1992) 195.
85 A. A. Wragg, F. N. Bravo de Nahui, in Electrochemical Engineering and the Environment, *IChemE Symposium Series* No. 127, p. 141, Rugby, UK, 1992.
86 G. P. Power, I. M. Ritchie, in B. E. Conway, J. O'M Bockris (eds.): *Modern Aspects of Electrochemistry*, No. 11, Prentice Hall, New York 1975, p. 199.
87 R. S. Rickard, M. C. Fuerstenau, *Trans A.I.M.E.* **242** (1968) 1485.
88 Ch. Schlimm, E. Heitz, *Environmental Progress* **15** (1996) 37.
89 L. Hartinger: *Taschenbuch der Abwasserbehandlung*, vol. 1, Hanser Verlag, München 1976, pp. 54 – 57.
90 R. Weiner: *Die Abwässer der Galvanotechnik und Metallindustrie*,4th ed., Eugen G. Leuze Verlag, Saulgau 1973, pp. 301 – 305.
91 F. Nohse: "Elektrodialyse," in L. Hartinger (ed.): *Taschenbuch der Abwasserbehandlung*,vol. 2, Carl Hanser Verlag, München 1977, pp. 165 – 175.
92 H. Behret, H. Binder, R. Eggersdorf, H. J. Hampel. A. Köhling, *Ber. Bunsenges. Phys. Chem.* **83** (1979) 1094 – 1097.
93 H. Binder, H. Behret, *DECHEMA Monogr.* **97** (1984) 289 – 303.
94 F. Linnhoff, *DECHEMA Monogr.* **97** (1984) 305 –307.
95 S. Itoi, J. Nakamura, T. Kawahara, *Desalination* **32** (1980) 383 – 389.
96 D. C. Johnson, N. Popović, J. Feng, L. L. Houk, K. T. Kawagoe, The Electrochem. Society, Proc. Volume 95 – 26, 176 – 188 (1996).
97 Ch. Comminellis, C. Pulgarin, *J. Appl. Electrochemistry* **21** (1991) 703.
98 Ch. Comminellis, C. Pulgarin, *J. Appl. Electrochem.* **23** (1993) 108.
99 Ch. Comminellis, *IChemE Symposium Series 127* (1992) 189 – 201.
100 V. Smith De Sucre, A. P. Watkinson, *Can. J. Chem. Eng.* **59** (1981) 52.
101 H. Sharifian, D. W. Kirk, *J. Electrochem. Soc.* **133** (1986) 921.
102 Ch. Comminellis, *Gas Wasser Abwasser* **72** (1992) no. 11.
103 K. Scott, The 1994 IChemE Research Event, Vol. 1, 344 (1994).
104 K. Scott, The Electrochemical Society, Proc. Vol. 94 – 19, p. 51 (1994).
105 P. W. T. Lu, R. L. Ammon, *J. Electrochem. Soc.* **127** (1980) 2610.

106 T. Hunger, F. Lapique, A. Storck, *J. Appl. Electrochem.* **21** (1991) 588.
107 G. H. Kelsall, S. Saage, D. Brandt, *J. Electrochem. Soc.* **138** (1991) 117.
108 P. Meszaros *et al.*, *Hungarian J. Ind. Chem.* **12** (1984) 163.
109 M. Sudoh *et al.*, *J. Chem. Eng. Japan* **21** (1988) 198.
110 S. D. Fleischmann, R. A. Pierce, US-Report WRSC-MS-91–192, 180th Meeting of The Electrochemical Society, Phoenix Arizona, 1991.
111 C.E.A. France, private communication.
112 J. C. Farmer, F. T. Wang, R. A. Hawley-Fedder, P. R. Lewis, L. J. Summers, L. Foiles, *J. Electrochem. Soc.* **139** (1992) 654.
113 F. Steele, *Platinum Met. Rev.* **34** (1990) 10.
114 U. Leffrang, K. Ebert, K. Flory, U. Galla, H. Schmieder, *Conf. Separation Sci. & Techn.*, Gatlinburg, Tennessee, USA, 24. – 28. Oct. 1993.
115 R. D. Lide (eds.): *CRC Handbook of Chemistry and Physics*,73rd ed., "Chap. 8", CRC Press, Boca Raton 1992 – 1993, pp. 17 – 27.
116 W. J. Plieth, *Encyclopedia of Electrochemistry of the Elements*,Vol. 8, 440.
117 U. Galla, J. Bringmann, H. Schmieder, GDCh Monografie, Vol. 14, 270 (1998).
118 J. Bringmann, U. Galla, H. Schmieder, *5th International HCH and Pesticides Forum, Leioa*, Basque Country, Spain, 25 – 27 June, 1998.
119 J. Bringmann, K. Ebert, U. Galla, U. Leffrang, H. Schmieder, ASME Heat Transfer Division, HTD-Vol. 317–2, (1995) IMECE 289.
120 G. Kreysa, H.-J. Külps, *Chem.-Ing.-Tech.* **55** (1983) 58.
121 G. Kreysa, H.-J. Külps, *Ger. Chem. Eng.* **6** (1983) 352.
122 G. Kreysa, H.-J. Külps, C. Woebcken, *Dechema-Monographien* **94** (1983) 199.
123 G. Kreysa, *Dechema-Monographien* **109** (1987) 9.
124 G. Kreysa, *Chem.-Ing.-Tech.* **62** (1990) 357.
125 R. Rottmann, Fortschr.-Ber. VDI, Reihe 15, Nr. 111, VDI-Verlag, Düsseldorf 1993.
126 Lurgi Schnellinformation C 1217/12.76 (1976).
127 D. van Velzen, H. Langenkamp, A. Moryoussef, *J. Appl. Electrochem.* **20** (1990) 60.
128 CZ 153 372, 1974 (F. Strafelda, J. Krofta).
129 G. Kreysa, J. M. Bisang, W. Kochanek, G. Linzbach, *J. Appl. Electrochem.* **15** (1985) 639.
130 P. Iliev, I. Nikolov, T. Vitanov, E. Budevski, *J. Appl. Electrochem.* **22** (1992) 425.
131 D. Townley, J. Winnick, *Electorchim. Acta* **28** (1983) 389.
132 H. S. Lim, J. Winnick, *J. Electrochem. Soc.* **131** (1984) 562.
133 D. Weaver, J. Winnick, *J. Electrochem. Soc.* **134** (1987) 2451.
134 J. Winnick, in H. Gerischer, C. W. Tobias (eds.): *Advances in Electrochemical Science and Engineering*, Vol. 1, VCH-Verlagsgesellschaft, Weinheim, Germany 1990, p. 205.
135 T. Hibino, *J. Appl. Electrochem.* **25** (1995) 203.
136 M. Aurousseau, C. Roizard, A. Storck, F. Lapicque, *Ind. Eng. Chem. Res.* **35** (1996) 1243.
137 J. M. Nzikou, M. Aurousseau, F. Lapicque, *J. Appl. Electrochem.* **25** (1995) 967.
138 K. Jüttner, G. Kreysa, K.-H. Kleifges, R. Rottmann, *Chem.-Ing.-Tech.* **66** (1994) 82.
139 K.-H. Kleifges, Fortschr.-Ber. VDI, Reihe 15, Nr. 153, VDI-Verlag, Düsseldorf 1996.
140 F. Lapicque, M. Aurousseau, C. Roizard, A. Storck, P. Dyens, *Dechema-Monographien* **128** (1993) 487.
141 M. Aurousseau, T. Hunger, A. Storck, F. Lapicque, *Chem. Eng. Sci.* **48** (1993) 541.
142 C. G. Vayenas, S. Bebelis, S. Ladas, *Nature* **343** (1990) 625.
143 C. G. Vayenas, M. M. Jaksic, S. Bebelis, S. G. Neophytis, *Modern Aspects of Electrochemistry* **29** (1995) 57.
144 J. Nicole, D. Tsiplakides, S. Wodiunig, C. Comninellis, *J. Electrochem. Soc.* (1977) L 312.
145 D. Pletcher: *Industrial Electrochemistry*,Chapman and Hall, London-New York 1982, pp. 200 – 216.
146 J. P. Hoare, M. A. LaBoda: "Electrochemical Machining," *Compr. Treatise Electrochem.* **2** (1981) 399 – 520.
147 J. P. Hoare, M. A. LaBoda: "Electrochemical Machining," in E. Yeager, A. J. Salkind (eds.): *Techniques of Electrochemistry*,J. Wiley & Sons, New York-Chichester-Brisbane-Toronto 1978, pp. 48 – 141.
148 A. Rahmel, W. Schwenk: *Korrosion und Korrosionsschutz von Stählen*,Verlag Chemie, Weinheim-New York 1977, p. 63.

Further Reading

C. Comninellis, G. Chen: *Electrochemistry for the Environment*,Springer, New York, NY 2010.
C. H. Hamann, A. Hamnett, W. Vielstich: *Electrochemistry*,2nd ed., Wiley-VCH, Weinheim 2007.
R. Holze: *Experimental Electrochemistry*,Wiley-VCH, Weinheim 2009.
P. Schmuki, S. Virtanen: *Electrochemistry at the Nanoscale*, Springer, New York, NY 2009.
J. Wang: *Analytical Electrochemistry*,Wiley-VCH, Weinheim, 2006.
T. G. Willard: *Solid State Electrochemistry*,Nova Science Publishers, Hauppauge, N.Y 2009.
C. G. Zoski: *Handbook of Electrochemistry*,Elsevier Science, Amsterdam, 2007.